UNIVERSITATEA BABEȘ-BOLYAI

Facultatea de Fizică

Școala Doctorală de Fizică

PhD Thesis Summary

Transforming Aquatic Waste into Functional Materials: Insights into Adsorption, Environmental Remediation, and Circular Reuse Pathways

---

Ilirjana BAJAMA

Supervizor

Prof.dr. Simona PINZARU

Cluj-Napoca

2026

Abstract

This thesis investigates strategies for transforming aged crustacean shell waste into functional carbonate-based powders and evaluates their physicochemical, structural, and functional properties, with Raman spectroscopy and Surface-Enhanced Raman Scattering (SERS) as central analytical tools, complemented with additional methods such as IR, SEM-EDX, XRD and DLS.

Doing this we investigated either biogenic materials or water environments. The work combines biomaterial characterization with the detection and monitoring of pollutant biomolecules such as antibiotics, dyes, and pesticides. Waters are monitored through methods like physical and chemical, biological, high tech tools, monitoring networks, etc. SERS is also introduced as a sensitive tool for detecting, monitoring, and evaluating pollutant adsorption in wastewater, as well as for characterizing hypersaline lake waters. The research focuses on calcium carbonate-based biogenic materials derived from crustacean shells, valorized as sustainable and multifunctional resources within a circular economy framework. approximately 18 million tons of shell waste generated annually worldwide correspond to nearly 12 million cubic meters of material, a volume sufficient to create a mass comparable in surface area to Romania's Lake Tarnița under a 5–6 meter layer of shells.

The first chapter presents the scientific background, emphasizing water contamination by antibiotics, synthetic dyes, and heavy metals. Due to their persistence and toxicity in the environment, rapid and sensitive analytical methods are required. Spectroscopic tools and others are used and described on their necessity in our study. Raman and SERS are identified as effective techniques because of their molecular specificity and trace-level detection capability. This section explores the efficacy of biogenic carbonates in capturing water contaminants, employing SERS to characterize the molecular-level adsorption mechanisms and evaluate the material's potential for industrial wastewater treatment.

The second chapter describes the application of SERS for environmental water monitoring. A one-year monthly monitoring program of two hypersaline lakes evaluated physicochemical parameters (pH, electrical conductivity, salinity) and correlated them with Raman and SERS spectral data. This study, the first to apply SERS for long-term environmental monitoring, was published in two articles (Biosensors), covering both the cold and warm tourist seasons, the latter showing anthropogenic impacts on water properties.

The third chapter focuses on the preparation and characterization of biogenic

fine powders and their conversion into phosphate minerals. It provides a comprehensive characterization of biogenic carbonate, detailing its structural, physicochemical, and morphological properties through a multi-analytical approach using Raman, IR, DLS, SEM-EDX, and XRD techniques. This chapter also investigates the chemical transformation of aged biogenic calcite into phosphate minerals, detailing the mechanisms of mineral replacement and the resulting changes in the material's structural and surface properties.

The fourth chapter further develops SERS as an advantageous method for studying pollutants in natural waters and introduces the novel use of biogenic carbonate as an adsorbent. Case studies included methylene blue, crystal violet, doxycycline hyclate, and the commercial copper-based pesticide Champ 77. Calibrated ball-milled biogenic powders proved to be efficient adsorbents for these contaminants. Another biogenic adsorbent is onion epidermal membrane, successfully implemented as a biogenic adsorbent scaffold, where Raman spectroscopy served to monitor the adsorption of pollutants.

Overall, the thesis demonstrates that marine biogenic materials can be sustainably repurposed as multifunctional resources, serving as remediation adsorbents. By integrating fundamental spectroscopic research with real-environment applications, the work provides original contributions to biogenic material reuse, pollutant capture, water protection, and circular bioeconomy strategies.

Introduction

The increasing demand for industrial production, rapid urbanization, and intensification of agriculture over the last century has generated critical challenges for environmental sustainability. One of the most pressing problems is the growing presence of pollutants in aquatic systems, ranging from dyes and heavy metals to pharmaceutical residues such as antibiotics [1–3]. These compounds are often highly persistent, resistant to natural degradation, and capable of bioaccumulating in organisms, thereby posing risks to ecosystems and human health [4–6]. In particular, antibiotics like doxycycline, and industrial dyes including methylene blue and crystal violet have been repeatedly detected in surface waters, sediments, and wastewater effluents [7–10]. The accumulation of such contaminants calls for efficient and cost-effective strategies for their detection, monitoring, and removal.

At the same time, the global seafood industry generates vast amounts of biogenic waste every year, especially in the form of crustacean shells (from crabs, shrimps, and lobsters). It is estimated that millions of tons of these shell wastes are produced annually, much of which ends up discarded in landfills or coastal areas, leading to secondary environmental burdens [11,12]. However, this so-called "waste" is actually a renewable resource, rich in calcium carbonate ($CaCO_3$), chitin, proteins, and carotenoid pigments such as astaxanthin [13–15]. These unique features make crustacean shells attractive raw materials within the framework of the blue bioeconomy, offering opportunities for valorization into functional biogenic carbonates and other value-added products [16,17].

Biogenic carbonates derived from shells typically occur in different polymorphs, including calcite, aragonite, vaterite, and amorphous calcium carbonate (ACC) [18–20]. Their hierarchical microstructure and porosity enable remarkable adsorption properties, while the embedded organics contribute to bioactivity and chemical complexity [21]. As a result, shell-derived powders have been proposed for diverse applications, ranging from biomedical engineering and drug delivery to catalysis and environmental remediation [22–24]. Nonetheless, to harness these capabilities effectively, it is crucial to understand how mechanical and chemical processing affects the mineral–organic framework. For instance, techniques such as ball milling can increase surface area and reactivity but may also induce amorphization or partial phase transitions [25–27].

A central aim of this thesis is to explore the transformation of aged crustacean shell waste into functional powders, with a focus on their physicochemical properties and their interaction with pollutants in aqueous systems. Special attention is devoted to spectroscopic characterization, particularly Raman spectroscopy and Surface-Enhanced Raman Scattering (SERS). Raman spectroscopy, based on the inelastic scattering of light, is a powerful tool for probing the vibrational modes of molecules, providing detailed insights into both organic and inorganic phases [28–30]. In the case of biogenic carbonates, Raman allows the identification of calcite and aragonite peaks, as well as signals from chitin and carotenoids [31,32]. Importantly, Raman spectroscopy is non-destructive and requires little to no sample preparation, making it highly suitable for complex natural materials [33] In environmental studies, SERS has been applied to detect dyes, antibiotics, pesticides, and heavy metals with high sensitivity and selectivity [34–36]. Combining biogenic carbonates with SERS thus offers a promising dual strategy: the materials act as adsorbents for pollutants, while SERS provides a powerful detection platform to monitor interactions and removal efficiency.

Crustacean shells aged under natural conditions were subjected to controlled milling procedures, producing powders of different particle sizes and crystallinities. These were characterized using a combination of X-ray diffraction (XRD) to assess crystallographic phases, Fourier-transform infrared spectroscopy (FT-IR) to analyze functional groups, dynamic light scattering (DLS) to evaluate particle size distributions, and scanning electron microscopy with energy-dispersive X-ray spectroscopy (SEM-EDX) to investigate morphology and elemental composition.

The pollutants chosen as case studies in this thesis represent three important categories: (i) antibiotics (doxycycline hyclate), which are widely used in veterinary and human medicine and persist in wastewater [37,38]; (ii) dyes (methylene blue and crystal violet), synthetic compounds used in textiles, paper, and medical diagnostics, often found in industrial effluents [39,40] and (iii) copper-based fungicides such as Champ 77 were investigated due to their heavy-metal content and environmental relevance [41]. By focusing on these pollutants, the study addresses both pharmaceutical and industrial contaminants, thereby reflecting real-world water pollution scenarios.

By integrating fundamental characterization with applied environmental testing, this research contributes to both materials science and environmental engineering. It demonstrates how natural waste resources can be converted into functional materials and how advanced spectroscopy can deepen our understanding of their properties and interactions. In doing so, the thesis supports global efforts to promote sustainable reuse of biogenic waste, develop eco-friendly remediation technologies, and advance the blue bioeconomy.

Thesis aim and scope

The growing demand for sustainable materials has increased interest in the reuse of marine biogenic resources. Crustacean shells, a major byproduct of the seafood industry, represent an abundant yet underutilized source of biominerals, organic

macromolecules, and pigments. 18 millions of tons are discarded annually, creating environmental burdens while overlooking their potential for value-added applications in environmental remediation, biomedicine, and materials science [42,43].

This thesis investigates strategies for transforming aged crustacean shell waste into functional carbonate-based powders and evaluates their physicochemical, structural, and functional properties, with Raman spectroscopy and Surface-Enhanced Raman Scattering (SERS) as central analytical tools. A primary objective is to determine how calibrated ball milling and subsequent treatments influence crystallinity, structural integrity, and preservation of organic components, enabling the reuse of these materials as low-cost sustainable sorbents and as precursors for advanced functional systems. Raman is emphasized for its non-destructive and mineral–organic sensitivity, while SERS enhances trace-level detection and real-time monitoring of adsorption processes. Functional testing in model wastewater systems containing methylene blue, crystal violet, doxycycline hyclate, and copper-based fungicides evaluates adsorption efficiency, pollutant–powder interactions, and removal mechanisms under realistic conditions [44–46]. SERS-based monitoring offers mechanistic insight into pollutant dynamics and demonstrates how spectroscopic tools can guide remediation strategies. Beyond environmental applications, the thesis explores biomedical implications. The preservation of carotenoids and organic matrix components suggests potential for antioxidant-enriched biomaterials, while conversion of biogenic carbonates into calcium phosphate phases such as brushite and hydroxyapatite highlights their suitability for bone substitutes and drug delivery platforms [47,48].

Overall, the thesis contributes to blue bioeconomy and circular sustainability principles by converting marine biowaste into functional materials. By integrating structural analysis, environmental remediation, and biomedical exploration, it

provides a multidisciplinary framework for valorizing biogenic carbonates and advancing sustainable technologies for water purification and pharmaceutical applications.

Future Needs and Applications

This research opens several directions for future development:

- Water treatment: Using ball-milled biogenic carbonate as a cost-effective adsorbent for dyes, antibiotics, and heavy metals in wastewater.
- Biomedical uses: Developing drug delivery systems and bone graft materials from converted calcium phosphates.
- Circular economy: Transforming food industry waste into high-value products, aligning with sustainability goals.
- Spectroscopic monitoring: Applying Raman and SERS as real-time, portable techniques for environmental monitoring and material analysis.

Structure of the Thesis

This doctoral thesis develops advanced Raman and Surface-Enhanced Raman Scattering (SERS) methods for the valorization of aquatic biogenic materials as efficient adsorbents for water pollutants. Calcium carbonate-based materials derived from crustacean shells are investigated as sustainable resources within a circular economy framework, combining structural characterization with pollutant detection and remediation strategies.

Chapter I presents the scientific background on water contamination by persistent pollutants such as antibiotics, synthetic dyes, and heavy metals. Raman spectroscopy and SERS are introduced as rapid and sensitive analytical techniques for trace-level detection. This section explores the efficacy of biogenic carbonates in capturing water contaminants, employing SERS to characterize the molecular-level adsorption mechanisms and evaluate the material's potential for industrial wastewater treatment.

Chapter II describes a one-year SERS-based monitoring program of two hypersaline

lakes. Physicochemical parameters (pH, electrical conductivity, salinity) were correlated with Raman and SERS spectral data to evaluate seasonal and anthropogenic influences. The study, published in two Biosensors articles, demonstrates the feasibility of long-term environmental monitoring using SERS. My contribution focused on data collection and analysis.

Chapter III focuses on the preparation and characterization of biogenic powders obtained through calibrated ball milling and their functionalization with silver nanoparticles. The materials preserved crystalline structure and natural pigments while exhibiting increased surface area and adsorption capacity. Their integration with metallic nanoparticles enabled the development of SERS-active substrates for trace pollutant detection.

Chapter IV investigates the application of these materials in pollutant remediation. Case studies include methylene blue, crystal violet, doxycycline hyclate, and the copper-based pesticide Champ 77. The ball-milled biogenic powders demonstrated efficient adsorption, while SERS analysis provided mechanistic insight into pollutant–carbonate interactions and copper-induced plasmonic "hot spot" formation.

Overall, the thesis demonstrates that marine biogenic waste can be transformed into multifunctional materials for environmental remediation and potential biomedical or veterinary applications, contributing to sustainable water management and the advancement of the blue bioeconomy.

1. Biogenic material and characterizing techniques

1.1 Fundamental Properties of Biogenic Powders

Biogenic powders are natural materials derived from biological structures formed through biomineralization or biopolymer assembly, including shells, bones, corals, diatom frustules, eggshells, and crustacean exoskeletons. After natural weathering or mechanical processing such as grinding and ball milling, these materials are converted into fine particulate forms while preserving their hybrid organic–inorganic character. This dual composition differentiates them from purely geological minerals and synthetic composites and underlies their increasing relevance in environmental remediation, materials science, and biomedical applications [49,50].

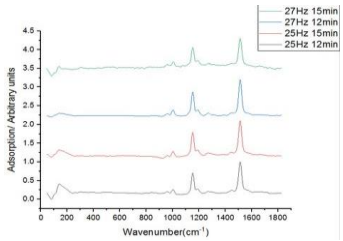

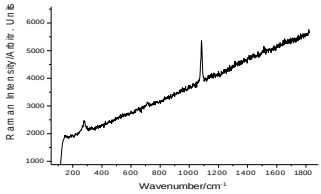

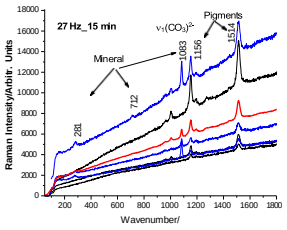

Figure 1.1.1 Typical Raman spectra of biogenic powder particles showing just pigments, typical spectra showing just mineral, and typical spectra showing mineral + pigments. Calcite is identified by its characteristic peaks at 1084 cm^{-1} (CO_3^{2-} symmetric stretching), 712 cm^{-1} (CO_3^{2-} bending), and 280 cm^{-1} (lattice vibrations). The characteristic Raman bands of astaxanthin were observed at 1512–1517 cm^{-1} (C=C stretching), 1154–1157 cm^{-1} (C–C stretching), and 1004– 1006 cm^{-1} (CH_3) [50].

The significance of biogenic powders arises from both their sustainability and the structural features inherited from their biological origin. Even after pulverization, powders may retain mineral polymorphs, residual organics, and structural motifs characteristic of biomineralization processes [51]. Figure 1.1.1 shows representative Raman spectra collected from different particles of the biogenic powder.

Marine derived materials such as mollusk shells, coral skeletons, and crustacean exoskeletons are among the most studied. These are typically calcium carbonate-based, dominated by calcite and/or aragonite [52]. The functional performance of biogenic powders depends strongly on their physical properties, particularly particle size, morphology, surface area, porosity, and crystallinity. Particle size is influenced by both the original biological structure and the processing method. Naturally fragmented materials may range from micrometers to millimeters, whereas mechanical milling can reduce particles to submicron or nanometer dimensions [54]. Prolonged ball milling generally decreases crystallite size, increases surface area, and enhances defect density. These changes promote higher chemical reactivity and dissolution rates, improving adsorption capacity and suitability for composite fabrication [55].

Overall, the combined physical properties particle size, morphology, porosity, crystallinity, color, density, optical response, and thermal behavior define the functional potential of biogenic powders. These parameters influence environmental

interactions, processing adaptability, and suitability for remediation, composite development, and biomedical applications.

From a chemical perspective, biogenic powders are intrinsically complex systems. Their mineral phases (calcium carbonate, calcium phosphate, or silica) coexist with organic macromolecules such as proteins, polysaccharides, lipids, and pigments. Trace elements including magnesium and strontium may be incorporated into the crystal lattice, modifying stability and solubility [56]. This intertwined organic–inorganic chemistry ultimately governs reactivity and functional performance, positioning biogenic powders as versatile and sustainable materials at the interface of biology and materials science.

1.2 Application of Biogenic Carbonates for Wastewater remediation Monitored by Raman Spectroscopy Techniques

Biogenic carbonates derived from shells, corals, eggshells, and crustacean exoskeletons are abundant natural biominerals formed through biologically controlled mineralization. When processed into powders, these materials provide a renewable, low-cost source of reactive $CaCO_3$ with hierarchical porosity and surface functionality that distinguish them from synthetic analogues [57–59]. Their hybrid mineral–organic nature makes them particularly suitable for wastewater remediation. Their remediation capacity is governed by surface chemistry and structural reactivity. Carbonate and hydroxyl groups enable ion exchange, electrostatic attraction, and surface precipitation, allowing the adsorption of organic pollutants, immobilization of heavy metals, and neutralization of acidic effluents. Milling further enhances performance by increasing surface area and defect density.

Raman spectroscopy offers a non-destructive and highly specific tool for characterizing these processes. Calcium carbonate exhibits a dominant ν_1 symmetric stretching band near 1085 cm^{-1}, with polymorph-specific lattice modes that allow discrimination between calcite, aragonite, and vaterite [60,61]. Raman also detects

preserved organic components such as proteins, chitin, and carotenoid pigments, reflecting the hybrid structure of biogenic powders.

During interaction with pollutants, Raman spectroscopy enables in situ monitoring of structural and chemical changes. Shifts or broadening of carbonate bands may indicate lattice distortion or ion exchange, while new vibrational features reveal precipitation of secondary phases. Heavy metals such as Pb^{2+}, Cd^{2+}, and Cu^{2+} can form metal–carbonate compounds detectable through changes in the carbonate spectral region [62]. Similarly, phosphate removal leads to formation of calcium phosphate phases (e.g., brushite or hydroxyapatite), accompanied by Raman bands near 950–1000 cm^{-1} [63]. Organic pollutant adsorption, including dyes and pharmaceuticals, is confirmed by the appearance of their characteristic vibrational bands superimposed on carbonate signals [64,65]. This direct spectroscopic evidence distinguishes surface adsorption from structural transformation. Surface-enhanced Raman spectroscopy (SERS) further increases sensitivity by integrating biogenic carbonates with plasmonic nanoparticles (Ag or Au). In such systems, the carbonate acts as the sorbent while metallic nanoparticles create electromagnetic "hot spots" that amplify Raman signals, enabling detection at nanomolar levels and providing insight into molecular binding configurations [66].

Raman techniques also allow evaluation of structural stability and reusability. Acidic conditions may induce carbonate dissolution, reflected by reduced ν_1 intensity or appearance of bicarbonate features [67]. Repeated adsorption–desorption cycles can modify crystallinity or reduce organic signals, highlighting the importance of regeneration strategies [68].

Overall, biogenic carbonates represent sustainable alternatives to conventional sorbents. Their abundance, biodegradability, and multifunctional surface chemistry, combined with Raman and SERS monitoring, enable simultaneous remediation and molecular-level analysis. This integration supports the development of efficient and adaptive wastewater treatment strategies based on renewable materials.

1.3 SERS for Demonstrating Adsorption of Water Pollutants

Surface-Enhanced Raman Spectroscopy (SERS) is a highly sensitive method for detecting water pollutants by amplifying Raman signals using plasmonic nanoparticles, typically silver or gold. Adsorption onto these substrates enhances otherwise weak molecular signals, allowing confirmation of pollutant binding and providing information on molecular orientation and interaction mechanisms.

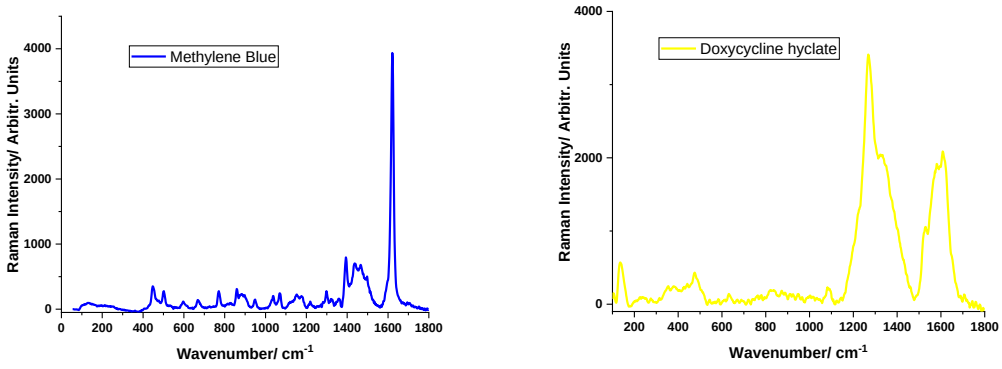

(a) (b)

Figure 1.3.1 Raman spectra of dye methylene blue (a) and doxycycline hyclate (b)

Biogenic carbonates functionalized with metallic nanoparticles act as dual-function systems, combining adsorption capacity with signal amplification through electromagnetic "hot spots." Organic dyes(Fig. 1.3.1.(a) and (b) shows the Raman spectra of two of them), pesticides, and pharmaceuticals exhibit characteristic vibrational bands upon adsorption, while time-dependent SERS measurements enable evaluation of adsorption kinetics alongside UV–Vis analysis. Although heavy metals are Raman-inactive, their immobilization can be inferred from indirect spectral changes related to metal–carbonate complex formation.

Reliable interpretation requires control experiments and uniform nanoparticle dispersion to ensure reproducibility. Overall, SERS offers high sensitivity, molecular specificity, and real-time monitoring, making SERS-functionalized biogenic.

2. SERS technique for environmental waters analysis

2.1 Case Study: Hypersaline Lakes at Cojocna — SERS Monitoring of Organic/Inorganic Balance

The Cojocna resort area (Cluj County, Romania) contains two hypersaline lakes (L1 and L2), formed from collapsed salt mines filled by groundwater. Although traditionally used for balneotherapy, their molecular composition has been little explored. Molnár et al. (2024) performed a pilot SERS monitoring study during the cold season (November–April) to minimize tourist influence and focus on natural variations [69].

Water samples were collected monthly in triplicate from the surface (~15 cm) and at one-meter depth, alongside in situ pH and conductivity measurements. The study hypothesized that SERS spectral features, particularly pigment-related bands, reflect microbial activity, while silver nanoparticle aggregation (driven by halides) indicates inorganic composition. The intensity ratio between the 245 cm^{-1} Ag–Cl band and the 1512 cm^{-1} β-carotene band (I_{245}/I_{1512}) was used as a semi-quantitative indicator of the inorganic/organic balance in the lakes.

2.1.1. What is in the Water? Major Components and Their Spectral Fingerprints

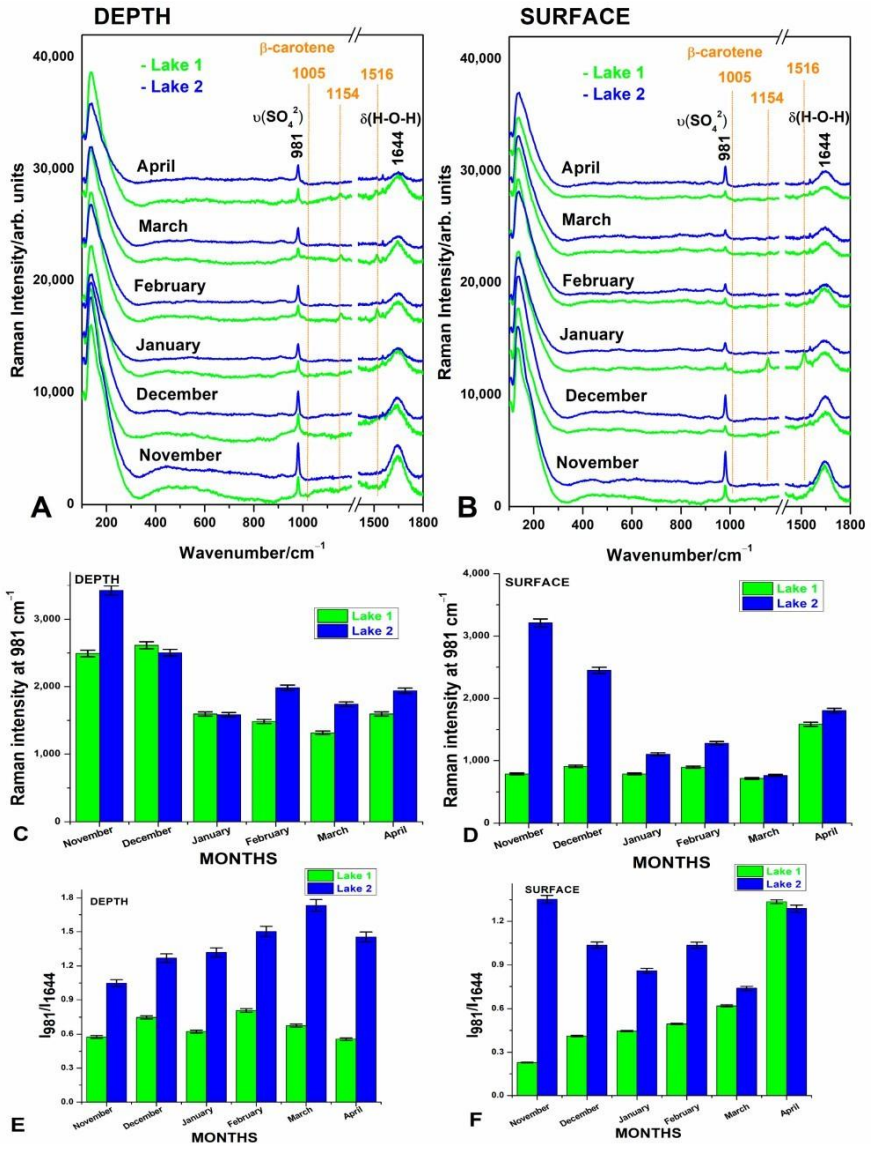

Figure 2.1.1.1. The in situ measured pH and electrical conductivity of salt waters from Lake 1 and Lake 2 at 1-meter depth (A,C) and at surface (B,D) during winter months from November 2022 to April 2023. Error bars represent a percentage of data values. The color legend always corresponds to green for Lake 1 and blue for Lake 2, as indicated on each graph. Error bars represents 1.94 % of value. Figure taken from the paper Molnár, C.; Drigla, T.D.; Barbu-Tudoran, L.; Bajama, I.; Curean, V.; Cîntă Pînzaru, S. Pilot SERS Monitoring Study of Two Natural Hypersaline Lake Waters from a Balneary Resort during Winter-Months Period.

Winter monitoring (November 2022–April 2023) showed clear physicochemical

differences between Lake 1 and Lake 2 (Figure 2.1.1.1). Lake 1 exhibited consistently higher pH values, indicating more alkaline conditions, while conductivity trends reflected distinct ionic compositions. Surface waters were slightly more variable than deeper layers due to atmospheric influence, whereas deeper waters remained more stable. The low overall error (1.94%) confirms measurement reliability (Molnár et al., 2024). Raman spectra identified sulfate ions (979 cm^{-1}), chloride-related aggregation effects, and carbonate bands, consistent with mineral-rich hypersaline waters (Figure 2.1.1.2) [70].

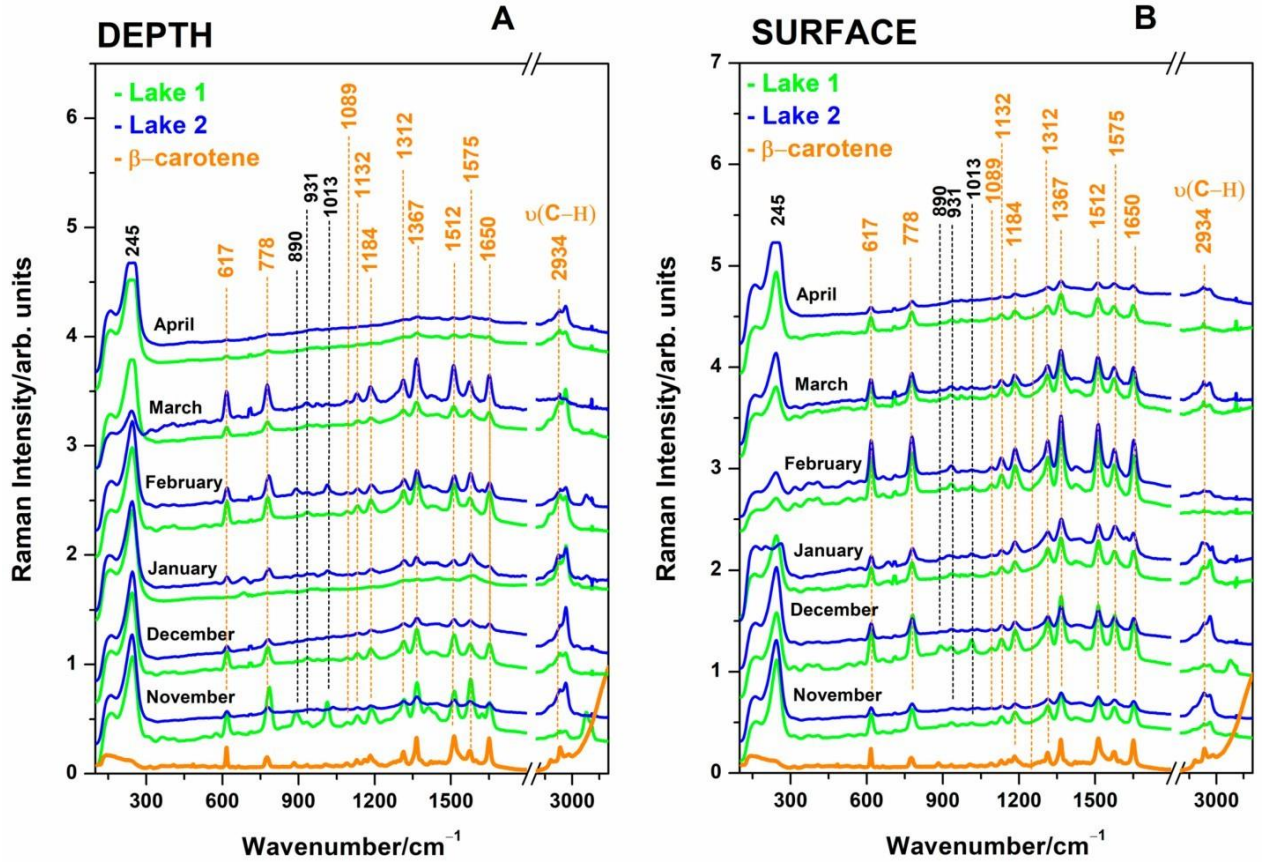

Figure 2.1.1.2. The SERS spectra collected from the salt waters of Lake 1 and Lake 2 from 1 m depth (A) and surface (B) waters over the six-month winter period, as indicated in each spectrum. Orange is shown for comparison in the SERS spectrum of pure β-carotene dissolved in ethanol solution, with SERS final concentration of 0.27 μM. Figure taken from the paper Molnár, C.; Drigla, T.D.; Barbu-Tudoran, L.; Bajama, I.; Curean, V.; Cîntă Pînzaru, S. Pilot SERS Monitoring Study of Two Natural Hypersaline Lake Waters from a Balneary

Resort during Winter-Months Period. Biosensors 2024, 14, 19. https://doi.org/10.3390/bios14010019 where I contributed in part to the obtaining and characterization of SERS spectra of environmental waters.

2.1.2 SERS evaluation of hypersaline waters in summer season monitoring program

Results

Raman Analysis of Sulfate

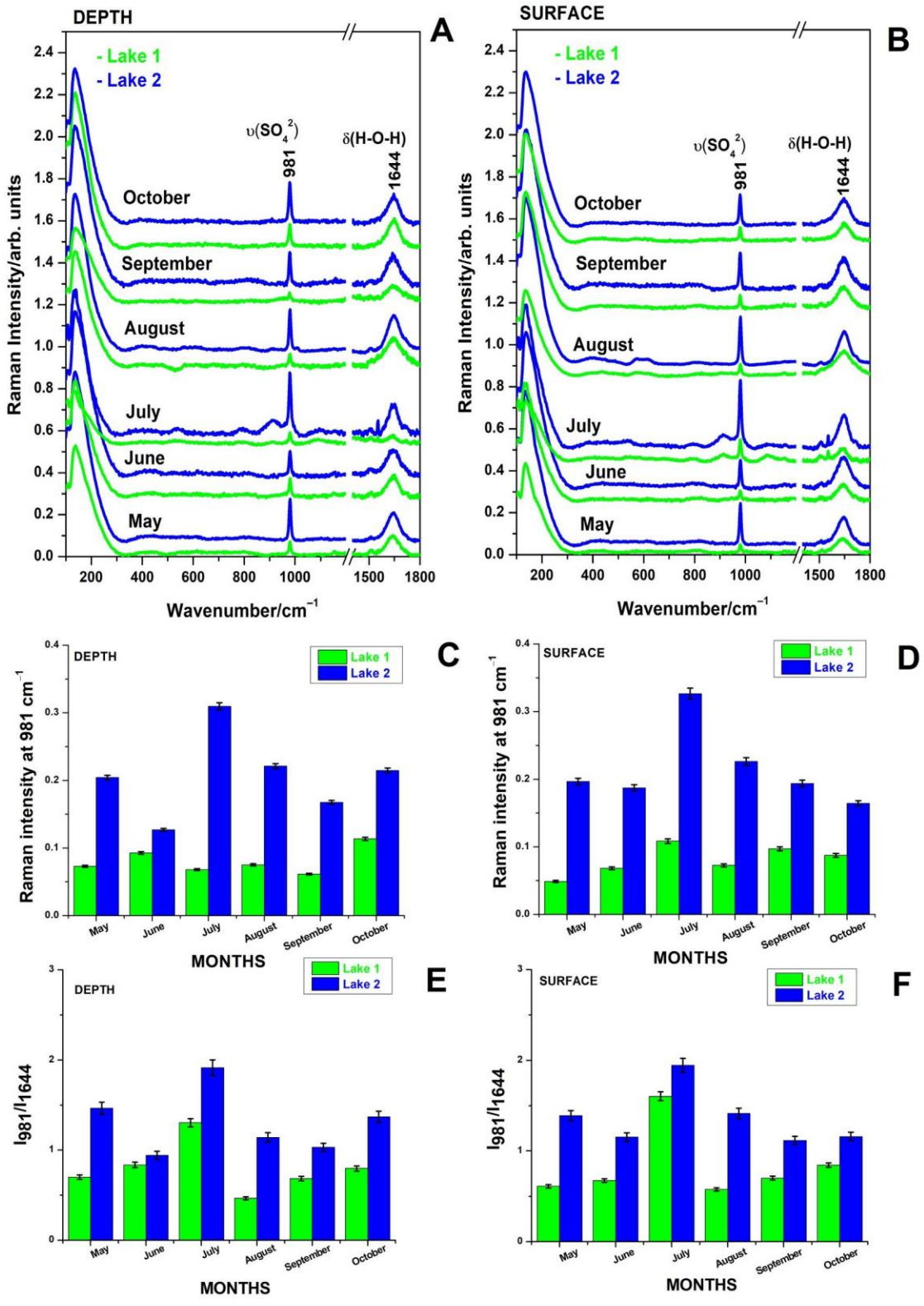

Figure 2.1.2.1 Raman spectra of lake waters showing sulfate band intensities at 981 cm^{-1} in L1 and L2 during summer monitoring. Molnár C, Maškarić K, Barbu-Tudoran L, Tămaș T, Bajama I, Pînzaru SC. SERS Detection of Environmental Variability in Balneary Salt

Lakes During Tourist Season: A Pilot Study. Biosensors (Basel). 2025 Oct 1;15(10):655. doi: 10.3390/bios15100655

SERS spectra (Fig. 2.1.2.1.) highlighted β-carotene peaks at 1512 cm^{-1}, indicative of cyanobacteria [71,72]. Variability in band intensity reflected seasonal cyanobacterial activity, with maxima in July and September. In addition, the Ag– Cl band at 245 cm^{-1} served as an indicator of chloride-induced nanoparticle aggregation, directly influenced by lake ion concentrations [73,74].

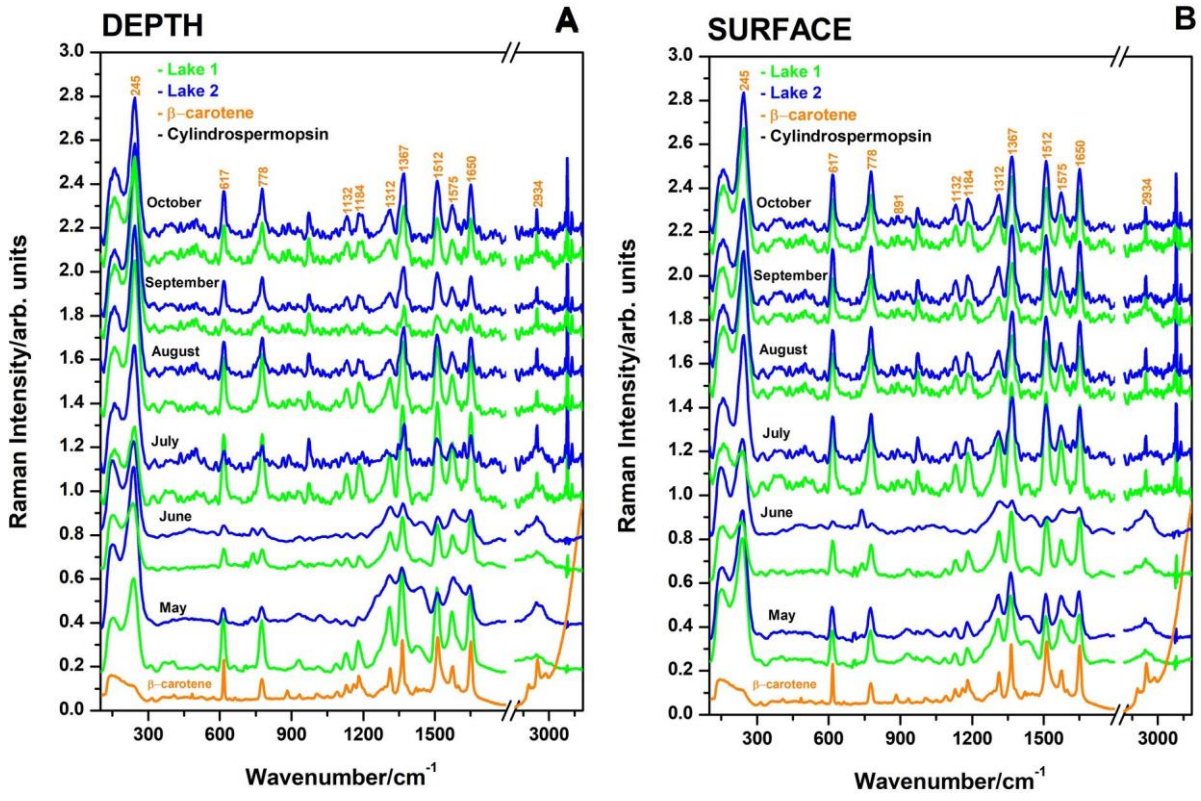

Figure 2.1.2.2. Representative SERS spectra from L1 and L2 waters, highlighting β- carotene at 1512 cm^{-1} and Ag–Cl at 245 cm^{-1}. Molnár C, Maškarić K, Barbu-Tudoran L, Tămaș T, Bajama I, Pînzaru SC. SERS Detection of Environmental Variability in Balneary Salt Lakes During Tourist Season: A Pilot Study. Biosensors (Basel). 2025 Oct 1;15(10):655. doi: 10.3390/bios15100655.

Discussion

Combined Raman and SERS analyses revealed that sulfate intensity strongly correlates with EC, confirming sulfate dominance in these hypersaline systems. L2

showed greater vertical stability, consistent with other sulfate-rich athalassohaline lakes. SERS detection of carotenoids indicated active cyanobacterial populations, with seasonal increases linked to temperature and evaporation. The Ag–Cl band (245 cm^{-1}) reflected chloride-driven nanoparticle aggregation and its interaction with microbial signals, demonstrating SERS sensitivity to both inorganic and organic components. No linear correlation between salinity and EC was observed at high ionic strength, confirming that conductivity alone is insufficient as a proxy for salinity. Comparative summer trends showed similar seasonal behavior in L1 and L2 but divergence at higher salinity, suggesting site-specific influences. Overall, integrating Raman/SERS with pH and EC measurements supports improved environmental monitoring and evidence-based balneary management.

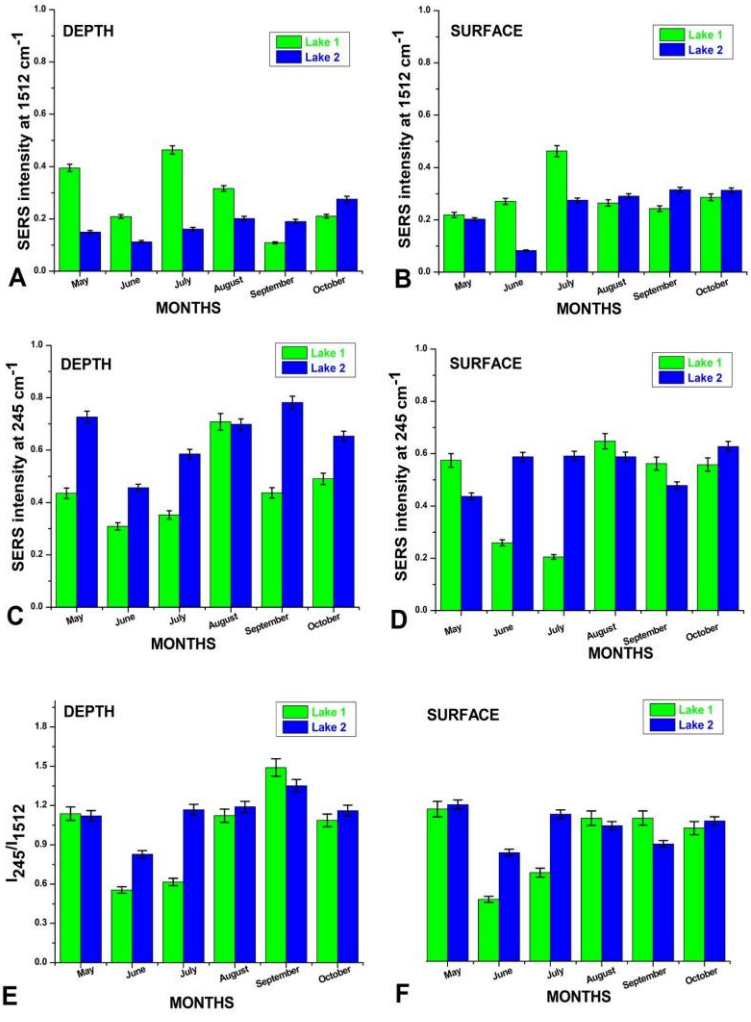

Figure 2.1.2.3. Comparative trends of salinity and conductivity in L1 and L2 during

summer monitoring, showing divergence at high salt concentrations. Molnár C, Maškarić K, Barbu-Tudoran L, Tămaș T, Bajama I, Pînzaru SC. SERS Detection of Environmental Variability in Balneary Salt Lakes During Tourist Season: A Pilot Study. Biosensors (Basel). 2025 Oct 1;15(10):655. doi: 10.3390/bios15100655

2.1.3. Comparison with Previous Winter Monitoring Study

This study examined the Cojocna hypersaline lakes during the summer tourist season (May–October 2023), characterized by high evaporation, increased microbial productivity, and anthropogenic influence. In contrast, Molnár et al. (2024) monitored the lakes during winter (October 2022–April 2023), when environmental conditions were more stable and tourist impact minimal [75]. Comparing these datasets highlights seasonal and human-driven variability.

Winter pH values ranged from 7.2 to 8.5, slightly higher in L1. In summer, pH showed greater variability (7.2–10.2), with more alkaline surface waters and peaks up to 10.2 in L1, reflecting stronger environmental forcing [75,76]. Similarly, winter EC values (110–120 mS/cm) were relatively stable, while summer EC reached 122.8 mS/cm (L1) and 120.8 mS/cm (L2), with higher surface values due to evaporation and biological activity [75,77].

Raman analysis consistently identified sulfate (981 cm^{-1}) as the dominant inorganic marker. While L2 maintained higher sulfate levels in both seasons, summer measurements showed amplified fluctuations, especially mid-season [75,78]. SERS results revealed stable β-carotene signals in winter, indicating persistent cyanobacteria, whereas summer showed pronounced peaks linked to microbial blooms [75,79]. The Ag–Cl band (245 cm^{-1}) appeared in both seasons but displayed greater variability in summer due to complex organic–inorganic interactions [75,80].

Statistically, winter conditions yielded stronger and more stable correlations, while summer data showed higher variability but greater sensitivity to ecological changes

[75,81]. Overall, winter provides a stable baseline, whereas summer amplifies physicochemical and biological dynamics. Integrating both datasets enables more comprehensive environmental and balneary monitoring.

3 Structural and functional evaluation of calibrated fine powders and their conversion into phosphate minerals

3.1 Ball Milling of Biogenic Carbonates: Structural, Physicochemical, and Functional Transformations

Ball milling is a mechanical process that reduces particle size, increases surface area, and modifies crystallinity and reactivity through repeated impacts between grinding media and powders [25–27]. By controlling milling time and frequency, reproducible powders can be obtained for targeted applications [54].

Structural changes are monitored using Raman (carbonate vibrations), FT-IR (organic residues), XRD (phase transitions), and SEM (morphology) [28–30,82–86].

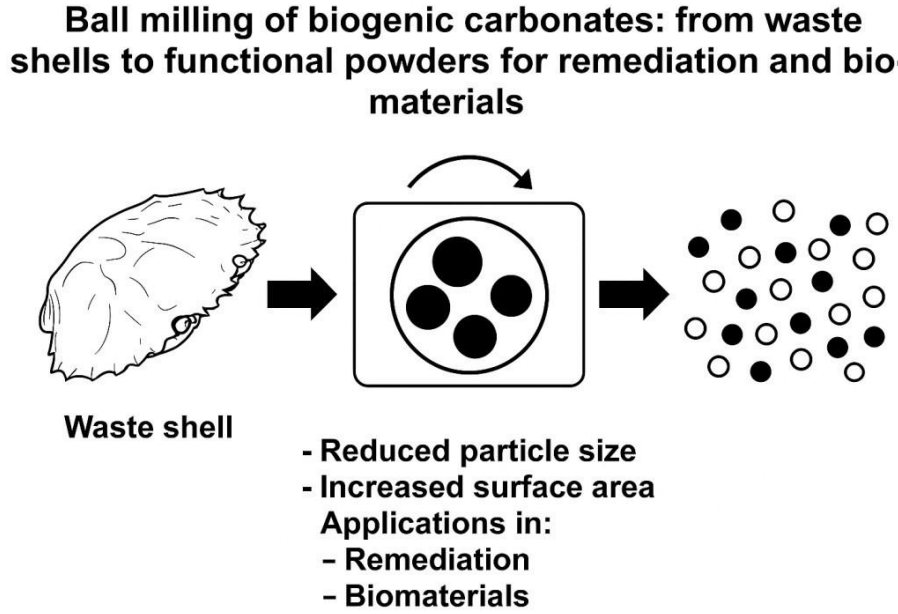

Figure 3.1.1. Schematic representation of ball milling applied to biogenic carbonates. The process reduces particle size, increases surface area, and modifies crystallinity, enabling transformation of shell-derived waste into functional powders for applications in

remediation, biomaterials, and sustainable material synthesis.

The shell fragments were milled into fine powders using a Retsch Mixer Mill MM 400 under controlled frequency and time conditions. Six grinding balls were used, with milling performed at 22–27 Hz for 12 or 15 minutes, generating four sample groups based on frequency and duration.

Results and Discussion

Surprisingly, despite changes in milling frequency and duration, optical microscopy did not reveal significant differences in particle sizes across the four powder groups. At all magnifications (5×, 20×, 50×, and 100×), the samples displayed comparable morphologies, characterized by irregularly shaped particles with broad size distributions ranging from approximately 1–2 μm up to several hundred micrometers (Fig. 3.1.2).

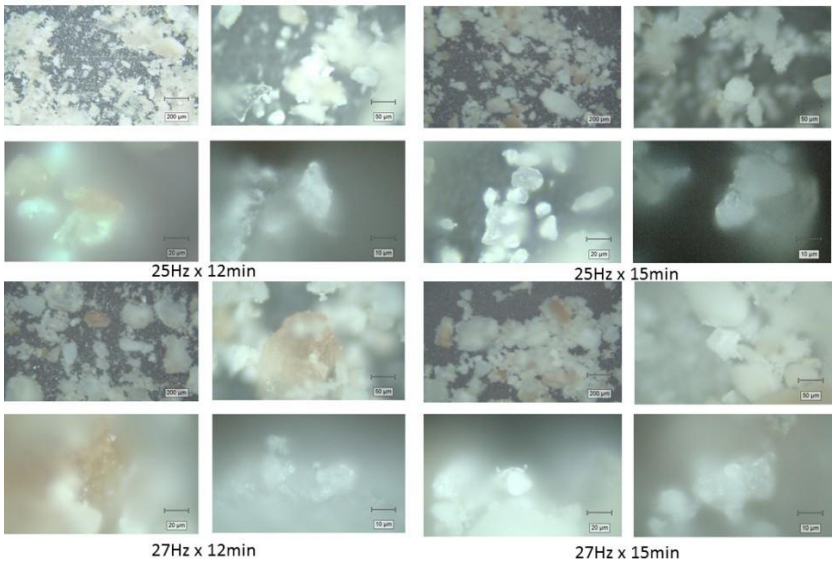

Figure 3.1.2. Representative optical microscopy images taken with the video camera of the Raman microscope prior to measurements, showing the morphology of the aged biogenic powder obtained under milling conditions 25 Hz for 12 min, 25 Hz for 15 mi ,
27 Hz for 12 min and 27 Hz for 15 min at 5×, 20×, 50×, and 100× magnifications objectives, respectively. Figure taken from: Bajama, I.; Maškarić, K.; Lazar, G.; Tamaş, T.; Costinaş, C.; Barbu-Tudoran, L.; Pinzaru, S.C. Aged Biogenic Carbonates from Crustacean

Waste: Structural and Functional Evaluation of Calibrated Fine Powders and Their Conversion into Phosphate Minerals. Materials 2025, 18, 5119. https://doi.org/10.3390/ma18225119

X-ray Diffraction (XRD) Analysis of Aged Powders

X-ray diffraction (XRD) was used to assess crystallinity and phase composition of the four milled powders (Fig. 3.2.3). All samples showed dominant calcite ($CaCO_3$) peaks (Fig. 3.1.4) at 2θ ≈ 23.1°, 29.4°, 31.6°, 36.1°, 39.4°, 43.1°, 47.5°, 48.5°, and 57.5°, confirming calcite as the main phase. Minor aragonite reflections (26.2°, 27.2°) and a broad band near 19.5° attributed to residual chitin were also detected. No significant differences between milling conditions were observed, indicating preservation of the crystalline structure after processing.

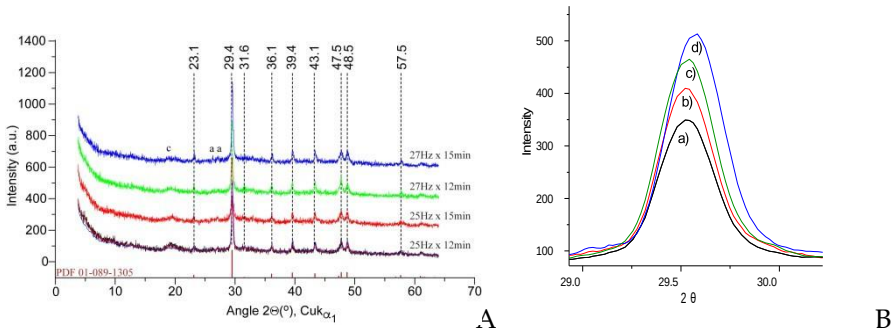

Figure 3.1.3. X-ray diffractograms A)of the biogenic powders milled under different conditions versus the magnesian calcite pattern from the 01-089-1305 PDF file [23]. Minor peaks of aragonite (a) and chitin) also occur. (B) Detail of the main calcite band at 29.4 angle is given to highlight the subtle band profile change with milling conditions. Figure taken from: Bajama, I.; Maškarić, K.; Lazar, G.; Tamaş, T.; Costinaş, C.; Barbu-Tudoran, L.; Pinzaru, S.C. Aged Biogenic Carbonates from Crustacean Waste: Structural and Functional Evaluation of Calibrated Fine Powders and Their Conversion into Phosphate Minerals. Materials 2025, 18, 5119. https://doi.org/10.3390/ma18225119

Fourier Transform Infrared Spectroscopy (FT-IR) Analysis of Powders

FT-IR spectroscopy was performed to analyze functional groups and possible chemical changes induced by milling. All four powder groups showed characteristic bands of calcium carbonate, mainly calcite and amorphous calcium carbonate (ACC) (Fig. 3.1.5). A shoulder at 1483 cm^{-1} indicated the presence of ACC and partially overlapped with organic bands from residual proteins and chitin. Overall, the spectra confirmed the hybrid mineral–organic composition and showed no major differences between milling conditions.

FT-IR spectra of all four powders showed characteristic bands of inorganic and organic components (Fig. 3.1.5). Strong carbonate signals appeared at 1401 cm^{-1} (asymmetric stretching) and 873 cm^{-1} (out-of-plane bending), confirming preserved calcite. A broad band at 3600–3200 cm^{-1} corresponded to O–H stretching from surface hydroxyls or adsorbed water, while peaks near 1650 cm^{-1} indicated residual chitin and protein (amide I), confirming the hybrid composition.

a)

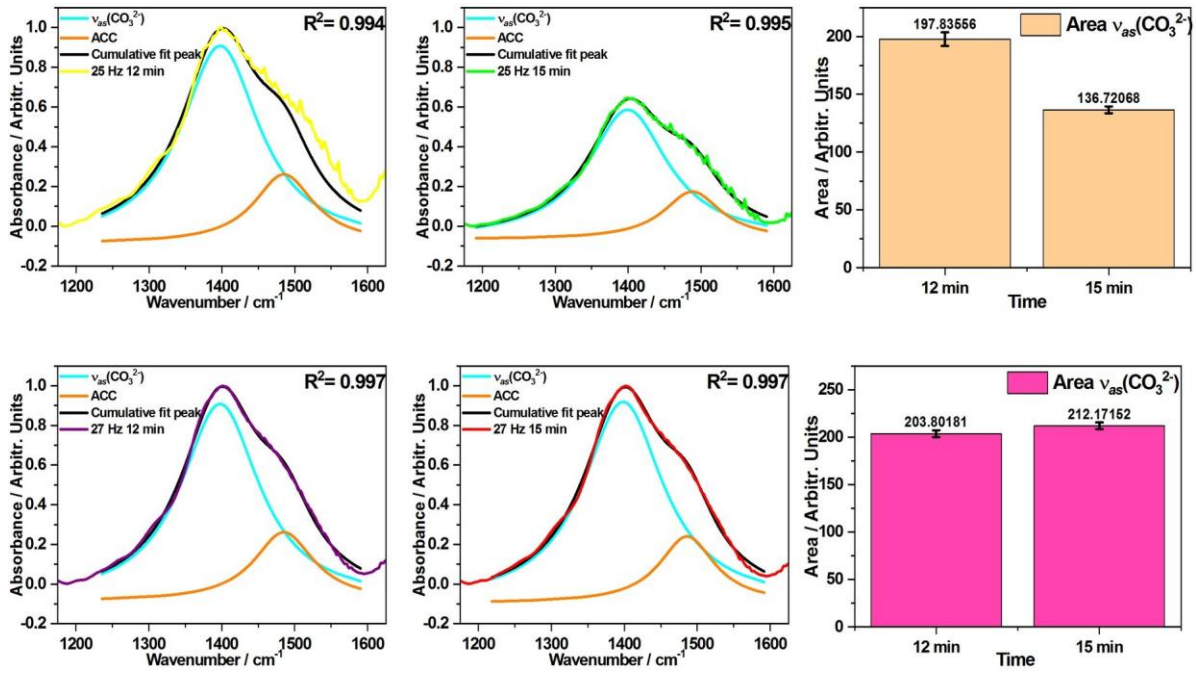

Figure 3.1.4. Deconvoluted IR band in the spectral range from 1200 to 1600 cm-1 comprising the main band assigned to the υ3 asym(CO32-) mode peaking at 1401 cm^{-1}, (red line) and

the amorphous calcium carbonate ACC (green line), changing in band features depending on time and frequency of ball milling. The comparative plot of the band area of the ν_3 asym(CO_3^{2-}) mode for two distinct milling times, under 25 Hz and 27 Hz frequencies, respectively are given in the right side. Highest band area was recorded for 27 Hz_15min. Figure taken from: Bajama, I.; Maškarić, K.; Lazar, G.; Tamaş, T.; Costinaş, C.; Barbu-Tudoran, L.; Pinzaru, S.C. Aged Biogenic Carbonates from Crustacean Waste: Structural and Functional Evaluation of Calibrated Fine Powders and Their Conversion into Phosphate Minerals. Materials 2025, 18, 5119. https://doi.org/10.3390/ma18225119

Micro-Raman Spectroscopy of Aged Powders

Raman spectroscopy (532 nm excitation) was used to analyze mineral phases and native pigments in the milled powders (Figs. 3.1.7). Carotenoid bands, particularly the C=C stretching at ~1513 cm^{-1}, were preserved in all powders and closely matched fresh shells and pure astaxanthin, indicating long-term pigment stability despite aging.

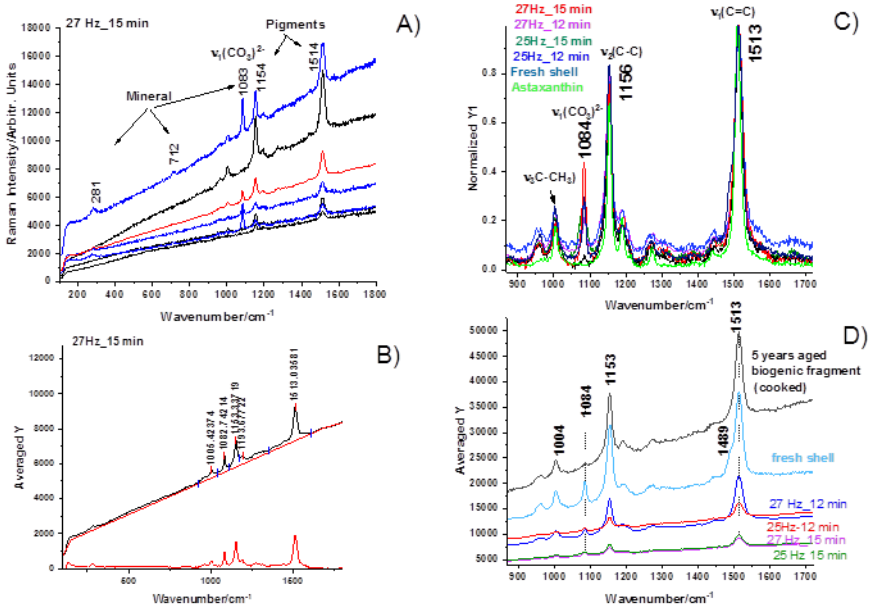

Figure 3.1.5. Micro-Raman spectra excited with 532 nm of the four powders resulted from the milling the aged biogenic material under different conditions: (A) Typical raw spectra (27 Hz for 15 min) and their averaged (red line) spectrum; particles with strong resonance Raman signal of carotenoids (black lines) and particles with stronger calcite bands (blue line) are observed; B) Raw Raman signal of random powder particle showing

both the calcite and astaxanthin pigment bands; C) Comparative, Raman signal of the four powders 25 Hz for 12 min, 25 Hz for 15 min, 27 Hz for 12 min, and 27 Hz for 15 min, compared to the RR signal of pure astaxanthin (green line) and with signal of fresh biogenic material (light blue line). D) Zoomed-in view of the 900-1700 cm-1 range of the averaged, raw spectra of the four powders, compared with the signal from an aged shell fragment (not milled) and one fresh fragment (light blue line), suggesting a slight broadening in the carotenoid band. Figure taken from: Bajama, I.; Maškarić, K.; Lazar, G.; Tamaş, T.; Costinaş, C.; Barbu-Tudoran, L.; Pinzaru, S.C. Aged Biogenic Carbonates from Crustacean Waste: Structural and Functional Evaluation of Calibrated Fine Powders and Their Conversion into Phosphate Minerals. Materials 2025, 18, 5119. https://doi.org/10.3390/ma18225119

Dynamic Light Scattering (DLS) Analysis

Particle size distribution was analyzed by Dynamic Light Scattering (DLS) on untreated dispersions to preserve the natural polydispersity of the ball-milled powders. The results (Fig. 3.1.8) showed two dominant peaks at ~255 nm and ~1290 nm, indicating coexistence of fine particles and larger aggregates. A third truncated peak near 5500 nm suggested the presence of very large particles prone to sedimentation.

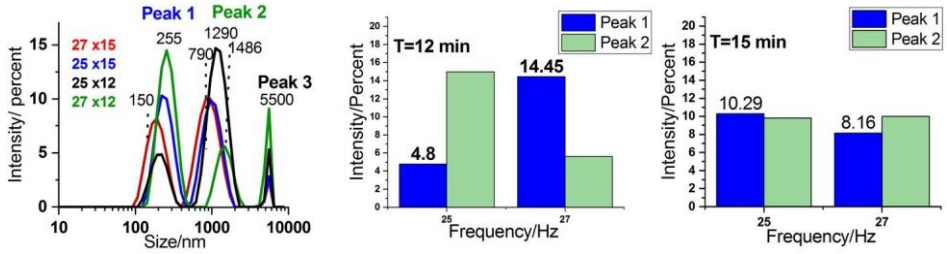

Figure 3.1.6. Dynamic Light Scattering (DLS) analysis of crab shell powders milled under various conditions:(a) Overlay of DLS spectra for all samples milled under different conditions: 27 Hz for 15 min, 25 Hz for 15 min, 25 Hz for 12 min, 27 Hz for 12 min. (b) Column plot showing the dependence of peak intensity on frequency for a milling time of 12 min and (c) 15 min. Figure taken from: Bajama, I.; Maškarić, K.; Lazar, G.; Tamaş, T.; Costinaş, C.; Barbu-Tudoran, L.; Pinzaru, S.C. Aged Biogenic Carbonates from Crustacean

Waste: Structural and Functional Evaluation of Calibrated Fine Powders and Their Conversion into Phosphate Minerals. Materials 2025, 18, 5119. https://doi.org/10.3390/ma18225119

3.2 Conversion of Aged Biogenic Calcite into Phosphate Minerals

The powders treated with phosphoric acid, following the stoichiometry for hydroxyapatite conversion, underwent an effervescent reaction when acid was added drop by drop to prevent loss of material. Optical microscopy showed rapid formation of brushite crystals on calcite surfaces, occurring almost instantaneously at ambient conditions.

Figure 3.2.1. Rapid conversion reaction when phosphoric acid is dropped into biogenic carbonate with instant formation of brushite crystals (hydrated calcium phosphate mineral). Figure taken from: Bajama, I.; Maškarić, K.; Lazar, G.; Tamaş, T.; Costinaş, C.; Barbu-Tudoran, L.; Pinzaru, S.C. Aged Biogenic Carbonates from Crustacean Waste: Structural and Functional Evaluation of Calibrated Fine Powders and Their Conversion into Phosphate Minerals. Materials 2025, 18, 5119. https://doi.org/10.3390/ma18225119

FT-Raman Analysis of Starting Material and Conversion Products

Using non-resonant 1064 nm excitation, FT-Raman spectra clearly resolved both mineral and organic components with minimal fluorescence. After phosphoric acid treatment, new phosphate bands at 986 and 879 cm^{-1} confirmed brushite ($CaHPO_4 \cdot 2H_2O$) formation (Fig. 3.2.2B). Importantly, carotenoid bands at 1151 and

1515 cm^{-1} persisted in the products, demonstrating preservation of bioactive pigments during transformation. Comparison of the phosphate (986 cm^{-1}) to carbonate (1083 cm^{-1}) intensity ratio showed increasing conversion efficiency with stronger milling, reflecting enhanced reactivity of smaller particles. Overall, brushite was the dominant phase in all samples, confirming successful conversion of aged biogenic calcite into calcium phosphate while retaining organic components.

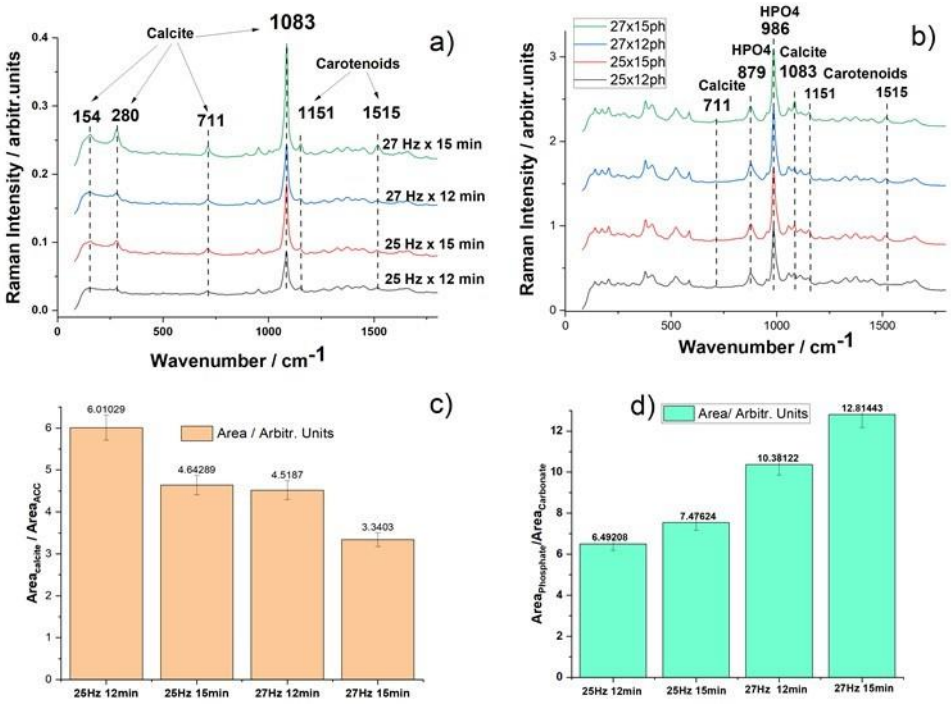

Figure 3.2.2. a) FT-Raman spectra of aged crustacean powders obtained with different milling times and frequencies; b) spectra of the conversion products showing the dominant bands of brushite (CaHPO4 x 2H2O), residual (trace) calcite and additional bands of carotenoids, as indicated; c) The plotted ratio of the calculated band area calcite/ACC in the starting powders, and d) ratio of the phosphate /carbonate in the final product (the band at 986 cm-1 of HPO4 and 1083 cm-1 of carbonate were used for calculation). Figure taken from: Bajama, I.; Maškarić, K.; Lazar, G.; Tamaş, T.; Costinaş, C.; Barbu-Tudoran, L.; Pinzaru, S.C. Aged Biogenic Carbonates from Crustacean Waste: Structural and Functional Evaluation of Calibrated Fine Powders and Their Conversion into Phosphate Minerals. Materials 2025, 18, 5119. https://doi.org/10.3390/ma18225119

X-ray Diffraction Analysis of conversion product

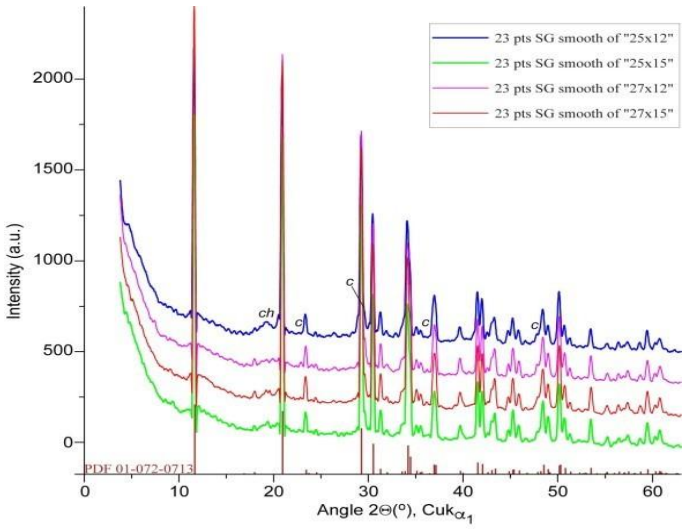

Figure 3.2.3. XRD patterns of biogenic calcite powders after the phosphoric acid treatment, and the pattern of brushite (calcium hydrogen orthophosphate dihydrate) from PDF file 01-0720713 (36). The marked peaks were attributed to chitin (ch) and unreacted calcite (c). Figure taken from: Bajama, I.; Maškarić, K.; Lazar, G.; Tamaş, T.; Costinaş, C.; Barbu-Tudoran, L.; Pinzaru, S.C. Aged Biogenic Carbonates from Crustacean Waste: Structural and Functional Evaluation of Calibrated Fine Powders and Their Conversion into Phosphate Minerals. Materials 2025, 18, 5119. https://doi.org/10.3390/ma18225119

XRD analysis (Fig. 3.2.3) confirmed the transformation of biogenic calcite into brushite ($CaHPO_4 \cdot 2H_2O$), evidenced by the disappearance of calcite peaks and the appearance of brushite reflections consistent with ICDD reference data. The conversion occurred efficiently across all samples through calcium–phosphate ion exchange, forming a stable crystalline phase without significant amorphization. The sharp diffraction peaks indicate preserved crystallinity, advantageous for biomedical applications such as bone grafting. These findings demonstrate that aged biogenic calcite waste can serve as a sustainable precursor for functional phosphate biomaterials.

SEM-EDX Analysis

A comparative analysis of elemental ratios obtained from EDX measurements is

presented in figure 3.2.4. The data show the phosphorus-to-calcium (P:Ca) and calcium-to-carbon (Ca:C) ratios of the brushite products derived from powders milled at frequencies of 25 Hz and 27 Hz, with milling times of 12 and 15 minutes. The Ca:C ratios revealed a marked reduction in carbonate content, reflecting the progressive loss of residual calcite during the reaction. These results demonstrate that while milling frequency and time influenced the extent of residual carbon removal, the overall phosphate formation pathway remained consistent, yielding structurally and compositionally comparable brushite products.

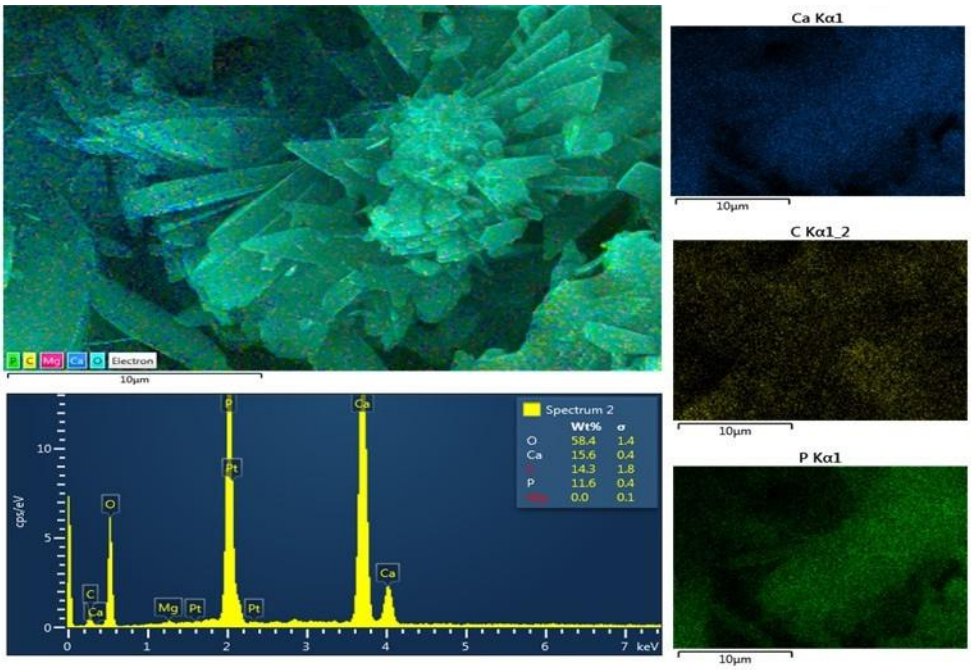

Figure 3.2.4. Recorded SEM image from phosphate mineral and EDX spectrum and maps of elements distribution (overlay and individual P, Ca and C) over the morphology of phosphate mineral from biogenic powder (25 Hz_12 min). Figure taken from: Bajama, I.; Maškarić, K.; Lazar, G.; Tamaş, T.; Costinaş, C.; Barbu-Tudoran, L.; Pinzaru, S.C. Aged Biogenic Carbonates from Crustacean Waste: Structural and Functional Evaluation of Calibrated Fine Powders and Their Conversion into Phosphate Minerals. Materials 2025, 18, 5119. https://doi.org/10.3390/ma18225119

Conclusion

Despite long-term aging, carotenoids embedded in the porous mineral matrix were remarkably preserved, retaining bioactive potential alongside mineral reactivity. Combined Raman, FT-IR, XRD, DLS, and SEM-EDX analyses showed that milling

induced only subtle, controllable changes, with calcite remaining the dominant.

The hybrid mineral–organic nature of the powders supports applications in pollutant adsorption and environmental remediation. Successful conversion into brushite further demonstrates their suitability as precursors for biomedical materials. Importantly, carotenoids remained stable even after phosphate transformation, suggesting potential for antioxidant-enriched biominerals. Overall, calibrated ball milling enables sustainable valorization of aged marine biowaste into functional materials aligned with circular and blue bioeconomy principles.

4 SERS analysis for removal of antibiotics, dyes and metals from wastewater treated with biogenic carbonate powder nanoparticles

4.1 Quantitative SERS control for wastewater and remediation using biogenic carbonate

The monitoring of pollutants in wastewater requires analytical methods that are both sensitive and capable of quantification under complex environmental conditions. While conventional chromatography and mass spectrometry are accurate, they are often time-consuming and costly. Surface-enhanced Raman spectroscopy (SERS) has emerged as a powerful alternative, enabling highly sensitive, selective detection and quantitative control when integrated with biogenic carbonate substrates [73, 74].

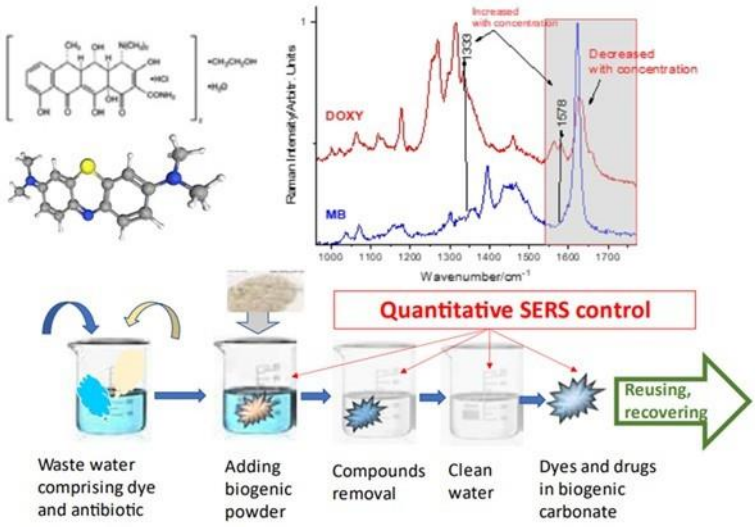

Fig. 4.1.1. Graphical design of the concept of empowering SERS as an effective tool for wastewater management and remediation using biogenic carbonate powders.

Their porous structures provide natural adsorption sites, while functionalization with silver or gold nanoparticles introduces the plasmonic "hot spots" necessary for SERS enhancement. Antibiotics like Doxycycline hyclate a broad-spectrum tetracycline that inhibits bacterial protein synthesis can disrupt essential microbial communities in water systems [68]. Similarly, synthetic dyes like Methylene blue reduce light penetration and photosynthetic activity, and can even produce toxic, carcinogenic aromatic amines. To evaluate the efficacy of biogenic materials, this study considers three representative pollutants:

Methylene blue: A model synthetic dye and photosensitizer.

Doxycycline hyclate: A broad-spectrum antibiotic representing pharmaceutical persistence.

Champ 77 (WG): A copper-based fungicide/bactericide used to inhibit pathogen growth on crops.

4.2 Doxycycline hyclate and Methylene blue absorption in porous biogenic carbonate

Materials and methods

Biogenic carbonate was obtained from crab shells through washing, drying, and high-energy ball milling to achieve a uniform particle size distribution. Doxycycline hyclate (DOXY) and methylene blue (MB) were selected as model pollutants. Raman measurements were performed using a Renishaw InVia Reflex spectrometer equipped with a 532 nm laser, initially on solid DOXY and aqueous MB solutions. In figure 4.2.1. it is shown the materials used. To investigate adsorption and release behavior, pellets were prepared using 3.68 g of biogenic carbonate. DOXY pellets contained approximately 93 mg of adsorbed antibiotic, while DOXY+MB pellets incorporated 52 mg of DOXY together with adsorbed MB. Raman, FT-IR, and XRD analyses confirmed that only calcite signals were detected in the solid pellets, indicating successful adsorption of the pollutants within the porous biogenic matrix.

Release kinetics were monitored in distilled water over seven hours, with supernatant samples collected every 30 minutes for Raman analysis. Changes in the characteristic Raman bands of DOXY and MB were used to quantify release profiles, retention capacity, and potential interactions between the pollutants and the sustainable biogenic carrier.

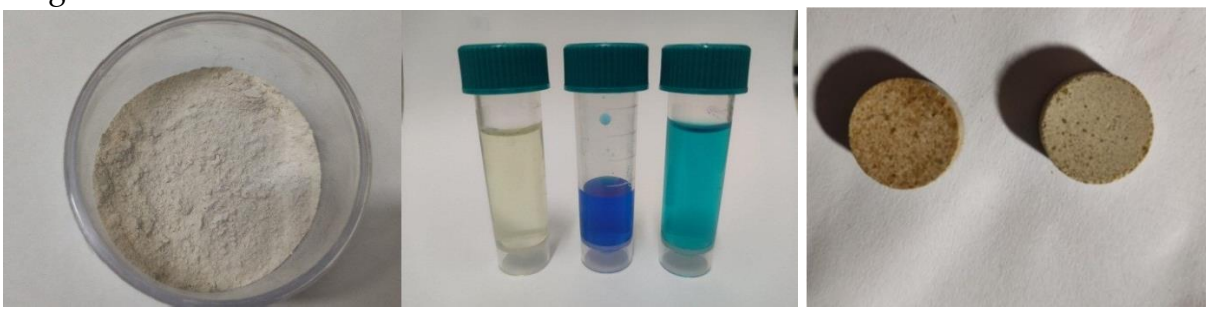

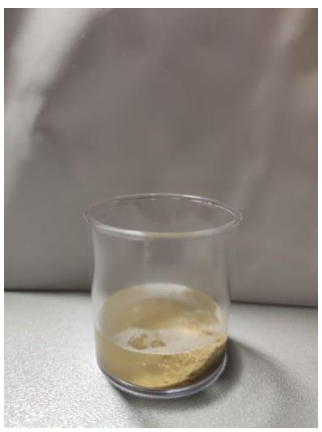

Figure 4.2.1 a) Fresh prepared biogenic powder; b) three solutions respective DOXY 10%, MB 10^{-3}; DOXY 10%+MB 10^{-3}c) DOXY+MB pellet and DOXY pellet; d) pellet diluted in water; e)Spectrometer Renishaw InVia Reflex Raman

Results and discussion

Fourier Transform Infrared Spectroscopy (FT-IR) Analysis of tablets loaded with Doxy, MB in biogenic powder

FT-IR analysis was performed to evaluate the structural features and molecular interactions in tablets composed of biogenic carbonate loaded with doxycycline (DOXY) and methylene blue (MB). The pristine biogenic carbonate exhibited characteristic calcite bands at 712, 873, and 1415 cm^{-1}, which remained unchanged in all tablet formulations, confirming preservation of the carbonate structure after loading. No distinct vibrational bands corresponding to DOXY or MB were observed in either the DOXY-only or DOXY+MB tablets, indicating that the active compounds were not surface-accessible but rather confined within the porous carbonate matrix.

The crushed DOXY+MB tablet showed only minor spectral variations, suggesting limited exposure of encapsulated compounds while still lacking clear DOXY or MB signatures.

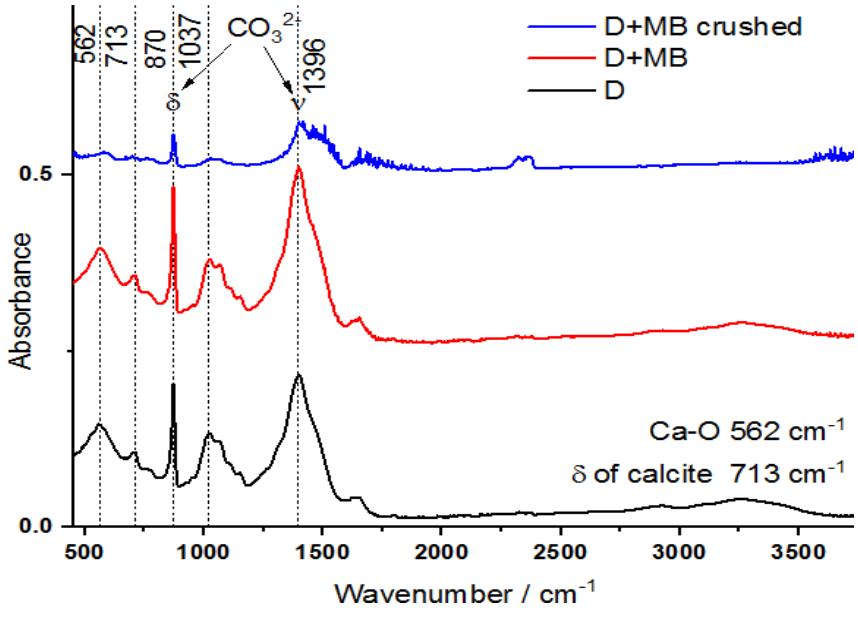

Figure 4.2.2 FT-IR spectra of tablets of biogenic carbonate loaded with doxycycline (D, black), doxycycline mixed with methylene blue (D+MB, red), and the crushed mixture (D+MB crushed, blue). Characteristic absorption bands are Ca–O stretching at 562 cm^{-1}, the δ bending mode of calcite at 713 cm^{-1}, carbonate vibrations at 870 and 1037 cm^{-1}, and the asymmetric stretching of CO_3^{2-} at 1396 cm^{-1}.

The releasing of the active compounds form tablets

The release behavior of doxycycline (DOXY) and methylene blue (MB) from biogenic carbonate tablets was investigated by monitoring their characteristic SERS signals in aqueous solution over 7–8 h. DOXY showed prominent bands at 1333 and 1578 cm^{-1}, with rapid release occurring within the first hour, indicating efficient desorption from the porous carbonate matrix. In contrast, MB exhibited a weak signal at 1623 cm^{-1} throughout the experiment, suggesting slower release.

For DOXY+MB tablets, the presence of MB affected the spectral detection of DOXY, suppressing its signals during the initial stages of release, while distinct DOXY bands became visible only after approximately 6 h. Maximum signal intensities were reached after ~35 min in 10 mL suspension and ~60 min in 5 mL suspension, demonstrating a dependence of release kinetics on solution volume.

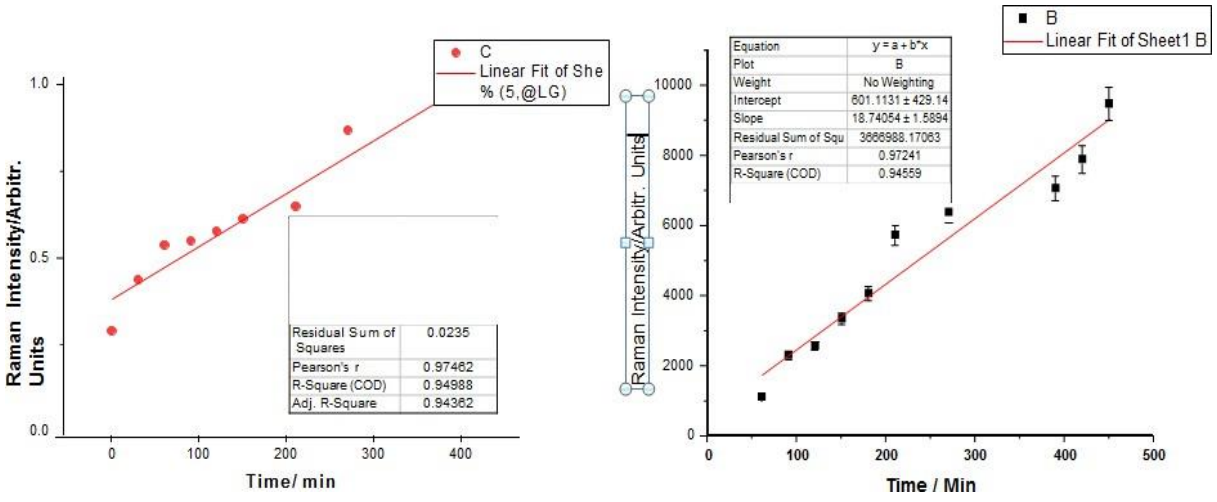

(a) (b)

Figure 4.2.3 (a) Doxy SERS intensity band at 1333 cm-1 in consecutive probes of released

solution in 7 hours experiments of tablet suspension in water, using batches of 10 µl solution added to 500 µl AgNPs. (b) Doxy+MB SERS intensity band at 1324 cm-1 in consecutive probes of released solution in 7 hours experiments of tablet suspension in water.

Conclusions

This study demonstrates the potential of crab shell-derived biogenic carbonate as a multifunctional material for the adsorption and controlled release of active compounds. FT-IR analysis confirmed the successful incorporation of doxycycline (DOXY) and methylene blue (MB) while preserving the calcite structure of the carrier, indicating effective encapsulation within its porous network.

SERS monitoring revealed time-dependent release of both compounds, with DOXY producing stronger signals than MB. In dual-loaded systems, the delayed and weaker detection of MB suggested competitive interactions influencing release kinetics.

4.3 Multiplexed SERS for wastewater treatment utilizing highly adsorbent biogenic powders to eliminate environmentally realistic mixtures comprising inorganic heavy metals, antibiotics and dyes

The simultaneous presence of antibiotics, dyes, and heavy metals in wastewater poses a significant environmental challenge due to their persistence, toxicity, and mutual interactions. These contaminants can affect each other's adsorption, mobility, and bioavailability, complicating both monitoring and remediation processes. For example, antibiotics such as doxycycline may form complexes with metal ions, while dyes can compete for available adsorption sites.

Understanding these interactions is crucial for designing efficient treatment strategies for multi-contaminant systems. In this regard, biogenic materials obtained from natural waste sources offer a sustainable alternative, providing porous structures suitable for pollutant adsorption and interaction studies. Such materials support the

development of environmentally friendly wastewater treatment technologies while enabling assessment of remediation performance.

Materials and methods

Biogenic powders were produced by controlled ball milling at 25 Hz and 27 Hz for 15 min to evaluate the effect of milling frequency on powder properties. Composite pellets were then prepared containing 10% doxycycline hyclate, methylene blue, and the copper-based fungicide Champ 77, representing antibiotics, dyes, and heavy metal contaminants. Special attention was given to achieving homogeneous distribution of the active compounds within the porous biogenic matrix. The pellets were immersed in water and their release behavior was monitored over 9 hours under controlled conditions. Structural characterization confirmed that the combined approach enabled correlation between powder crystallinity and pollutant release performance.

Results

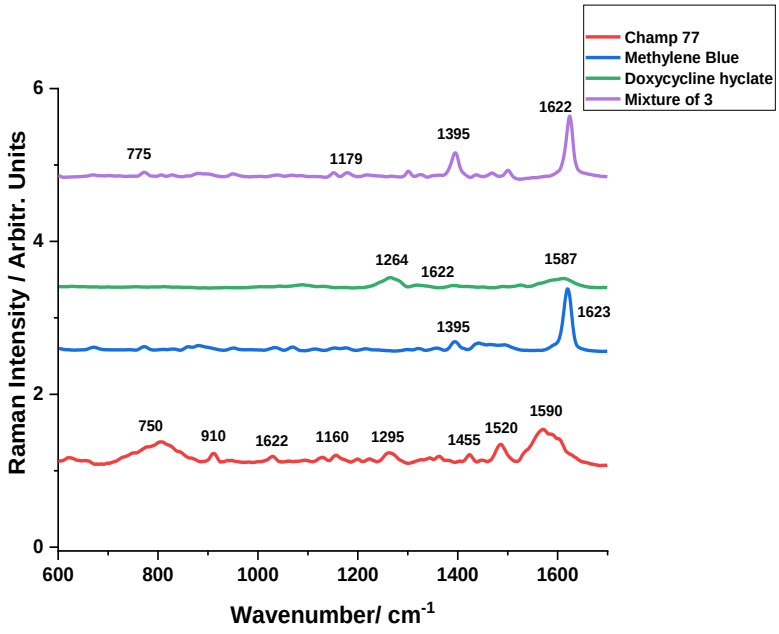

Figure 4.3.1 SERS spectra of Champ 77, Methylene blue , Doxycycline hyclate and their mixture Excitation: 633 nm for Champ 77 and Mix 3, 532nm for MB and Doxy

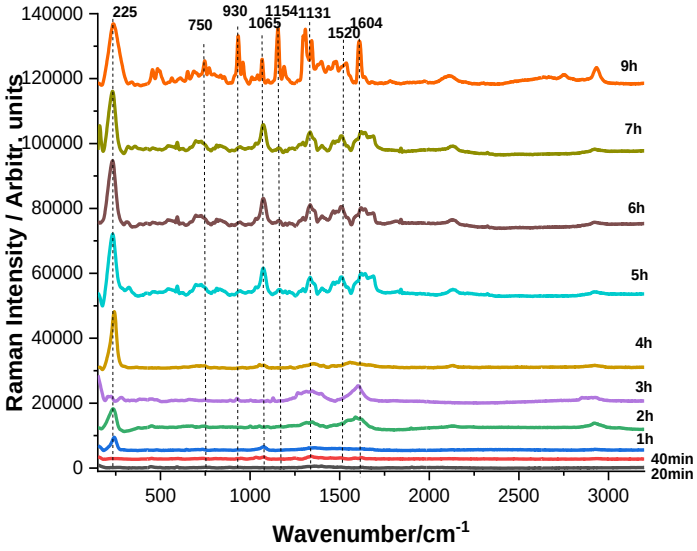

Figure 4.3.2 SERS release spectra of solution from the tablet formulation of biogenic powder 25Hz x 15min with pollutants: DOXY, MB and Champ 77. Excitation: 633 nm

SERS spectra of doxycycline hyclate, methylene blue (MB), and Champ 77, together with their mixtures, are presented in Figures 4.3.1–4.3.2. Release experiments performed with powders milled at 25 Hz and 27 Hz (15 min) revealed characteristic vibrational signatures of the compounds, with doxycycline monitored through bands at 1333 cm^{-1} (25 Hz) and 1345 cm^{-1} (27 Hz) during the 9-hour release period.

Doxycycline displayed prominent bands at 1085, 1153, 1262, 1436, 1578, and 1623 cm^{-1}, while MB showed a dominant peak at 1623 cm^{-1} with secondary features near 1396 and 1436 cm^{-1}. In the presence of Champ 77, doxycycline bands exhibited intensity variations and slight shifts, suggesting interactions with copper species, whereas MB remained spectrally stable. Spectra obtained at 25 Hz showed sharper and more intense features compared to 27 Hz, indicating enhanced signal quality and improved accessibility of active sites, although molecular interactions between the compounds remained consistent across milling conditions.

4.4.MB adsorption from another biogenic material, MB and Crystal Violet adsorption on 4 powders with different conditions

4.4.1 Raman spectroscopy techniques for monitoring of the MB recovery from waste waters using a biologic membrane

Onion epidermal membranes are simple, readily available plant-based materials with potential applications in environmental remediation and biosensing. Rich in cellulose, hemicellulose, and pectin, these biogenic structures possess characteristic molecular features that facilitate both structural characterization and adsorption studies. Previous research has demonstrated the effectiveness of onion-derived biomaterials and their carbonized forms in dye removal and filtration applications.

In this work, onion membranes were explored as a low-cost and sustainable platform for methylene blue adsorption from wastewater, while also providing information on the structural stability and adsorption properties of plant-based biological materials.

Methodology

Sample Preparation

Fresh onion bulbs were peeled to isolate the inner epidermal membrane, which was rinsed with distilled water, air-dried, and cut into uniform fragments for reproducible experiments. The membranes (0.656 g) were immersed in 30 mL of 1×10^{-4} M methylene blue (MB) solution under ambient conditions to allow dye adsorption onto the cellulose- and pectin-rich structure. Membranes were removed at defined intervals (12 h, 23 h, 36 h, 74 h, and 7 days) and gently dried before analysis to monitor the adsorption and interaction behavior over time.

Results

Optical microscopy revealed progressive morphological changes in the onion membrane during methylene blue exposure. After **12 h**, the membrane retained a

uniform cell structure, while **23 h** showed initial dye aggregation on the surface, indicating the onset of adsorption. Increased pigment accumulation at cell junctions was observed by **74 h**, and after **7 days** the membrane exhibited uniform and intense staining. These observations confirm gradual MB uptake with significant adsorption occurring after prolonged exposure.

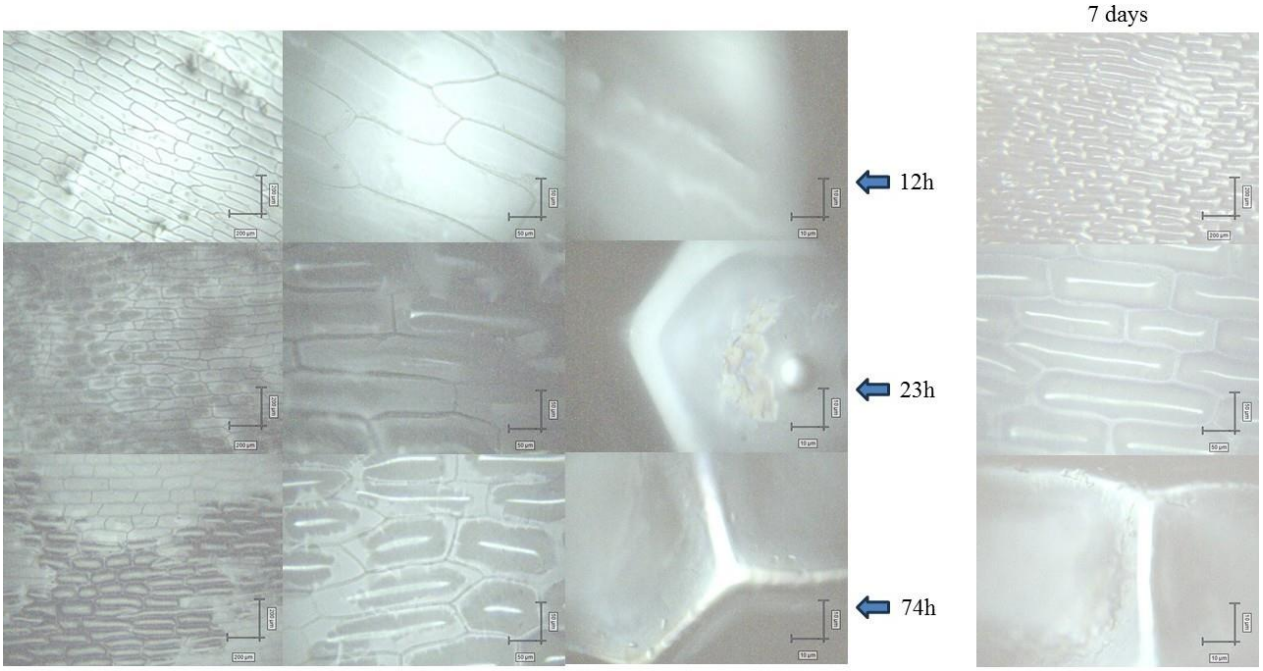

Figure 4.4.1.1. Onion membrane under microscope objectives: 5x, 20x and 100x for timing of 12h, 23h, 74h and 7 days

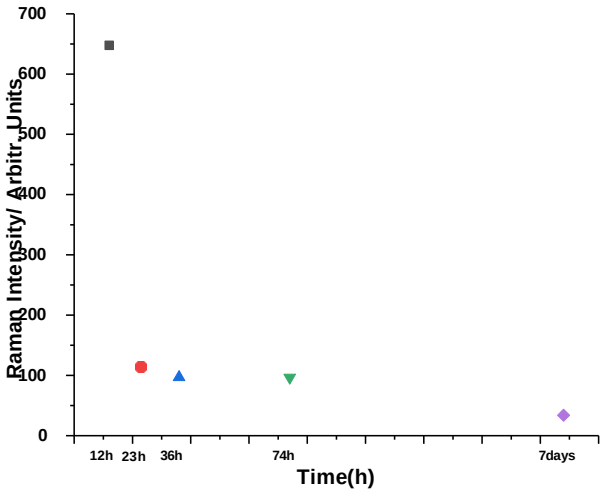

Fig. 4.4.1.2 Time evolution of the methylene blue Raman band at 1623 cm^{-1} measured

after 12 h, 23 h, 36 h, 74 h, and 7 days in biogenic membrane suspension.

Figure 4.4.1.2 illustrates the temporal evolution of the methylene blue (MB) Raman band at 1623 cm^{-1} during incubation in biogenic membrane suspension. The band at 1623 cm^{-1}, assigned to the aromatic C–C stretching vibration of MB, exhibited a progressive decrease in intensity over time. This trend reflects the gradual reduction in SERS enhancement as MB molecules, initially adsorbed at the membrane surface and accessible to plasmonic hot spots, became increasingly immobilized into the membrane matrix. These observations confirm that SERS can effectively monitor dye–membrane interactions and provide insights into the dynamic redistribution and stabilization of molecules within biogenic structures.

4.4.2 Crystal violet and MB adsorption on biogenic carbonate

Crystal violet (CV) and methylene blue (MB) are widely used cationic dyes that exhibit high environmental persistence and potential toxicity, making their removal from wastewater an important challenge. To evaluate dye adsorption, a mixed solution containing 0.8×10^{-5} M MB and 0.4×10^{-5} M CV was prepared and combined with biogenic carbonate suspensions obtained under different milling conditions (25 and 27 Hz for 12 and 15 min). Each experiment used 0.5 g of powder, corresponding to approximately 0.816 mg CV and 0.00128 mg MB per batch.

The mixtures were kept under static conditions at room temperature to mimic passive remediation systems. Spectroscopic analyses performed before and after treatment were used to assess adsorption efficiency and dye–carbonate interactions.

Results

On the first day, all samples displayed intense Raman bands characteristic of methylene blue and crystal violet, confirming the presence of adsorbed dye molecules on the biogenic carbonate surface. A pronounced reduction in signal intensity observed on the second day indicated efficient dye adsorption and possible

degradation processes, with adsorption performance improving at higher milling frequencies and longer milling times.

The powder processed at 27 Hz for 15 min exhibited the greatest signal suppression, consistent with enhanced adsorption resulting from increased surface area and reduced particle size. In contrast, the 25 Hz for 12 min sample retained slightly stronger dye signals. These findings demonstrate the effectiveness of biogenic carbonate powders in removing organic dyes and emphasize the importance of milling conditions in optimizing adsorption efficiency.

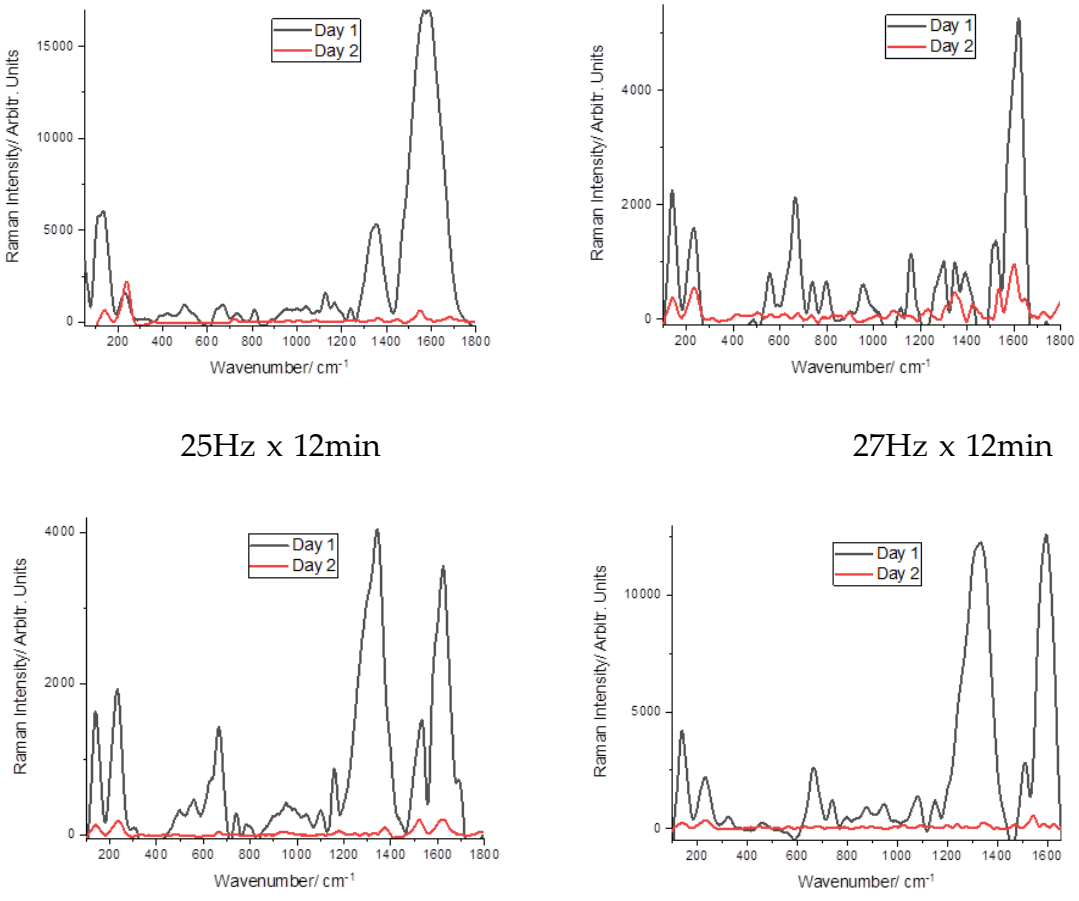

Figure 4.4.2.1. SERS spectra of methylene blue and crystal violet mixtures recorded for four different batches of biogenic carbonate powders prepared under calibrated ball milling conditions: (a) 25 Hz × 12 min, (b) 25 Hz × 15 min, (c) 27 Hz × 12 min, and (d) 27 Hz × 15 min. Each plot compares spectra collected after 1 day (black) and 2 days (red)

of exposure.

Conclusions and Outlook

This thesis demonstrated that aged crustacean shells represent a valuable source of biogenic carbonates with significant potential for environmental and biomedical applications. Although commonly treated as waste, these materials retain a complex composition of calcium carbonate, organic matrices, and carotenoid pigments that remain stable even after prolonged storage. Spectroscopic and structural analyses confirmed the preservation of the calcite phase and revealed the persistence of carotenoids, highlighting the protective role of the organic–inorganic framework and providing additional functional value linked to antioxidant properties.

Controlled ball milling introduced beneficial modifications, including reduced particle size and increased surface area, without compromising mineral integrity. These structural changes enhanced adsorption capacity and reactivity, demonstrating that mechanical processing can effectively tailor biogenic carbonates for targeted applications. The successful transformation of milled powders into brushite further confirmed their adaptability as biomaterial precursors, while the detection of retained organic components suggested the possibility of developing multifunctional phosphate materials with added bioactivity.

The environmental performance of the powders was validated through adsorption studies involving dyes, antibiotics, and copper-based compounds. Results showed efficient pollutant removal accompanied by spectroscopic evidence of molecular interactions, with milling conditions influencing adsorption efficiency through surface area variations. These findings support the use of crustacean-derived carbonates as low-cost, sustainable sorbents suitable for wastewater treatment and pollutant monitoring.

Overall, this work provides both scientific and practical contributions by demonstrating the structural resilience of aged shells, the tunability of their

properties through mechanical processing, and their multifunctional applicability as adsorbents and biomaterial precursors. While further studies are required to address scalability and performance in complex environments, the results establish a strong foundation for the circular valorization of shell waste. In conclusion, aged crustacean shells can be reinterpreted as a stable and adaptable resource capable of supporting sustainable material development, environmental remediation, and future biomedical innovation.

References:

[1] T. aus der Beek, F.-A. Weber, A. Bergmann, S. Hickmann, I. Ebert, A. Hein, and A. Küster, "Pharmaceuticals in the environment—Global occurrences and perspectives," Environ. Toxicol. Chem., vol. 35, no. 4, pp. 823 –835, 2016, doi: 10.1002/etc.3339.

[2] K. Kümmerer, "The presence of pharmaceuticals in the environment due to human use—Present knowledge and future challenges," J. Environ. Manage., vol. 90, no. 8, pp. 2354–2366, 2009, doi: 10.1016/j.jenvman.2009.01.023.

[3] B. Petrie, R. Barden, and B. Kasprzyk-Hordern, "A review on emerging contaminants in wastewaters and the environment: Current knowledge, understudied areas and recommendations," Water Res., vol. 72, pp. 3 –27, 2015, doi: 10.1016/j.watres.2014.08.053.

[4] A. B. A. Boxall, "Pharmaceuticals and personal care products in the environment: What are the big questions?," Environ. Health Perspect., vol. 122, no. 5, pp. 513–521, 2014, doi: 10.1289/ehp.1307667.

[5] S. R. Hughes, P. Kay, and L. E. Brown, "Global synthesis and critical evaluation of pharmaceutical data sets collected from river systems," Environ. Sci. Technol., vol. 47, no. 2, pp. 661–677, 2013, doi: 10.1021/es3030148.

[6] D. J. Lapworth, N. Baran, M. E. Stuart, and R. S. Ward, "Emerging organic contaminants in groundwater: A review of sources, fate and occurrence," Environ. Pollut., vol. 163, pp. 287–303, 2012, doi: 10.1016/j.envpol.2011.12.034.

[7] A. J. Watkinson, E. J. Murby, D. W. Kolpin, and S. D. Costanzo, "Antibiotic-resistant bacteria in sewage treatment plants: A novel pathway for resistance spread?," Water Res., vol. 43, no. 3, pp. 863–871, 2009, doi: 10.1016/j.watres.2008.11.021.

[8] R. Zhang, S. Tang, L. Wang, Z. Zhou, and Z. Guo, "Occurrence, sources, and risks of antibiotics in the environment," Crit. Rev. Environ. Sci. Technol., vol. 51, no. 22, pp. 2511–2545, 2021, doi: 10.1080/10643389.2020.1807452.

[9] C. G. Daughton and T. A. Ternes, “Pharmaceuticals and personal care products in the environment: Agents of subtle change?,” Environ. Health Perspect., vol. 107, suppl. 6, pp. 907–938, 1999, doi: 10.1289/ehp.99107s6907.

[10] L. Rizzo, et al., “Urban wastewater treatment plants as hotspots for antibiotic-resistant bacteria and genes spread into the environment,” Sci. Total Environ., vol. 447, pp. 345–360, 2013, doi: 10.1016/j.scitotenv.2013.01.032.

[11] FAO, The State of World Fisheries and Aquaculture. Rome: Food and Agriculture Organization of the United Nations, 2018.

[12] S. K. Kim and E. Mendis, “Bioactive compounds from marine processing byproducts – A review,” Food Res. Int., vol. 39, no. 4, pp. 383–393, 2006, doi: 10.1016/j.foodres.2005.10.010.

[13] L. Addadi, S. Raz, and S. Weiner, “Taking advantage of disorder: Amorphous calcium carbonate and its roles in biomineralization,” Adv. Mater., vol. 15, no. 12, pp. 959–970, 2003, doi: 10.1002/adma.200300381.

[14] H. Ehrlich, Biomimetic and Bioinspired Materials: Structure and Applications. Berlin: Springer, 2010.

[15] T. Nagai, N. Izumi, T. Ishii, T. Hattori, and N. Kanamori, “Preparation and characterization of chitin and chitosan from crab shell waste,” Polym. Degrad. Stab., vol. 91, no. 2, pp. 314–320, 2006, doi: 10.1016/j.polymdegradstab.2005.05.020.

[16] J. Venkatesan, et al., “Chitin and chitosan from marine organisms: A review,” Food Hydrocoll., vol. 38, pp. 24–30, 2014, doi: 10.1016/j.foodhyd.2013.11.003.

[17] J. Blau, “Blue bioeconomy—A new wave of innovation,” Mar. Policy, vol.123, p. 104310, 2021, doi: 10.1016/j.marpol.2020.104310.

[18] S. Weiner and P. M. Dove, “An overview of biomineralization processes and the problem of the vital effect,” Rev. Mineral. Geochem., vol. 54, no. 1, pp. 1–29, 2003, doi: 10.2113/0540001.

[19] N. Nassif, et al., “Amorphous and crystalline calcium carbonate nanoparticles:

Preparation, characterization, and application," J. Mater. Chem., vol. 15, no. 35–36, pp. 3628–3636, 2005, doi: 10.1039/b504465a.

[20] F. C. Meldrum and H. Cölfen, "Controlling mineral morphologies and structures in biological and synthetic systems," Chem. Rev., vol. 108, no. 11, pp. 4332–4432, 2008, doi: 10.1021/cr8002856.

[21] Z. Chen, et al., "Biomineralization inspired material design for environmental remediation," Acc. Chem. Res., vol. 49, no. 4, pp. 442 –451, 2016, doi: 10.1021/acs.accounts.5b00544.

[22] T. H. Silva, et al., "Marine origin collagens and its potential applications," Mar. Drugs, vol. 12, no. 12, pp. 5881–5901, 2012, doi: 10.3390/md12125881.

[23] Z. Li, et al., "Porous calcium carbonate microparticles as carriers for drug delivery," J. Mater. Chem. B, vol. 5, no. 18, pp. 3531–3541, 2017, doi: 10.1039/c7tb00346g.

[24] A. Arakaki, et al., "Biomineralization-inspired material synthesis," MRS Bull., vol. 40, no. 6, pp. 509–516, 2015, doi: 10.1557/mrs.2015.113.

[25] P. Baláž, Mechanochemistry in Nanoscience and Minerals Engineering.Berlin: Springer, 2008.

[26] C. Suryanarayana, "Mechanical alloying and milling," Prog. Mater. Sci., vol. 46, no. 1–2, pp. 1–184, 2001, doi: 10.1016/S0079-6425(99)00010-9.

[27] V. V. Boldyrev, "Mechanochemistry and mechanical activation of solids," Russ. Chem. Rev., vol. 75, no. 3, pp. 177–189, 2006, doi: 10.1070/RC2006v075n03ABEH001205.

[28]D. A. Long, The Raman Effect: A Unified Treatment of the Theory of Raman Scattering by Molecules. Chichester: Wiley, 2002.

[29] E. Smith and G. Dent, Modern Raman Spectroscopy – A Practical Approach. Chichester: Wiley, 2005.

[30] J. R. Ferraro, K. Nakamoto, and C. W. Brown, Introductory Raman Spectroscopy. 2nd ed. San Diego: Academic Press, 2003.

[31] J. De Gelder, K. De Gussem, P. Vandenabeele, and L. Moens, "Reference database of Raman spectra of biological molecules," J. Raman Spectrosc., vol. 38, no. 9, pp. 1133–1147, 2007, doi: 10.1002/jrs.1734.

[32] J. Jehlička and H. G. M. Edwards, "Raman spectroscopy as a tool for the non-destructive identification of organic minerals in the geological record," Org. Geochem., vol. 39, no. 4, pp. 371–386, 2008, doi: 10.1016/j.orggeochem.2007.11.004.

[33] P. Matousek and M. D. Morris, Emerging Raman Applications and Techniques in Biomedical and Pharmaceutical Fields. Springer Series in Optical Sciences, vol. 168. Berlin: Springer, 2010.

[34] M. Fan, G. F. S. Andrade, and A. G. Brolo, "A review on the fabrication of substrates for surface-enhanced Raman spectroscopy and their applications in analytical chemistry," Anal. Chim. Acta, vol. 1097, pp. 1 –29, 2020, doi: 10.1016/j.aca.2019.11.049.

[35] D. Cialla-May, et al., "Surface-enhanced Raman spectroscopy (SERS): Progress and trends," Anal. Bioanal. Chem., vol. 409, no. 27, pp. 641 –657, 2017, doi: 10.1007/s00216-017-0180-z.

[36] L. Guerrini and D. Graham, "Molecularly-mediated assemblies of plasmonic nanoparticles for surface-enhanced Raman scattering applications," Chem. Soc. Rev., vol. 41, no. 21, pp. 7085–7107, 2012, doi: 10.1039/c2cs35117a.

[37] K. Choi, D. Kim, J. Kim, and P. Kim, "Risk assessment of antibiotics detected in Korean aquatic environments," Ecotoxicol. Environ. Saf., vol. 71, no. 1, pp. 168–175, 2008, doi: 10.1016/j.ecoenv.2007.08.017.

[38] A. K. Sarmah, M. T. Meyer, and A. B. A. Boxall, "A global perspective on the use, sales, exposure pathways, occurrence, fate and effects of veterinary antibiotics in the environment," Chemosphere, vol. 65, no. 5, pp. 725 –759, 2006, doi: 10.1016/j.chemosphere.2006.03.026.

[39] T. Robinson, G. McMullan, R. Marchant, and P. Nigam, "Remediation of dyes in textile effluent: A critical review on current treatment technologies with a proposed alternative," Bioresour. Technol., vol. 77, no. 3, pp. 247 –255, 2001, doi: 10.1016/S0960-8524(00)00080-8.

[40] E. Forgacs, T. Cserháti, and G. Oros, "Removal of synthetic dyes from wastewaters: A review," Environ. Int., vol. 30, no. 7, pp. 953–971, 2004, doi: 10.1016/j.envint.2004.02.001.

[41] M. Komarek, V. Cadkova, D. Chrastny, F. Bordas, and J. Bollinger, "Contamination of vineyard soils with fungicides: A review of environmental and toxicological aspects," Environ. Int., vol. 36, no. 1, pp. 138–151, 2010, doi: 10.1016/j.envint.2009.09.007.

[42] T. aus der Beek, F.-A. Weber, A. Bergmann, S. Hickmann, I. Ebert, A. Hein, and A. Küster, "Pharmaceuticals in the environment—Global occurrences and perspectives," Environ. Toxicol. Chem., vol. 35, no. 4, pp. 823 –835, 2016, doi: 10.1002/etc.3339.

[43] K. Kümmerer, "The presence of pharmaceuticals in the environment due to human use—Present knowledge and future challenges," J. Environ. Manage., vol. 90, no. 8, pp. 2354–2366, 2009, doi: 10.1016/j.jenvman.2009.01.023.

[44] T. Robinson, G. McMullan, R. Marchant, and P. Nigam, "Remediation of dyes in textile effluent: A critical review on current treatment technologies with a proposed alternative," Bioresour. Technol., vol. 77, no. 3, pp. 247 –255, 2001, doi: 10.1016/S0960-8524(00)00080-8.

[45] E. Forgacs, T. Cserháti, and G. Oros, "Removal of synthetic dyes from wastewaters: A review," Environ. Int., vol. 30, no. 7, pp. 953–971, 2004, doi: 10.1016/j.envint.2004.02.001.

[46] M. Komarek, V. Cadkova, D. Chrastny, F. Bordas, and J. Bollinger, "Contamination of vineyard soils with fungicides: A review of environmental and toxicological aspects," Environ. Int., vol. 36, no. 1, pp. 138–151, 2010, doi:

10.1016/j.envint.2009.09.007.

[47] Z. Li, et al., "Porous calcium carbonate microparticles as carriers for drug delivery," J. Mater. Chem. B, vol. 5, no. 18, pp. 3531–3541, 2017, doi: 10.1039/c7tb00346g.

[48] A. Arakaki, et al., "Biomineralization-inspired material synthesis," MRS Bull., vol. 40, no. 6, pp. 509–516, 2015, doi: 10.1557/mrs.2015.113.

[49] L. Addadi and S. Weiner, "Biomineralization: Mineral formation by organisms," Angew. Chem. Int. Ed., vol. 31, no. 2, pp. 153–169, 1992, doi: 10.1002/anie.199201531.

[50] H. Ehrlich, Biological Materials of Marine Origin: Vertebrates. Dordrecht: Springer, 2010.

[51] J. R. Ferraro, K. Nakamoto, and C. W. Brown, Introductory Raman Spectroscopy, 2nd ed. San Diego: Academic Press, 2003.

[52] S. Mann, Biomineralization: Principles and Concepts in Bioinorganic Materials Chemistry. Oxford: Oxford University Press, 2001.

[53] T. Nagai, N. Izumi, and T. Ishii, "Preparation and characterization of chitin and chitosan from crab shell waste," Polym. Degrad. Stab., vol. 91, no. 2, pp. 314–320, 2006, doi: 10.1016/j.polymdegradstab.2005.06.020.

[54] C. Suryanarayana, "Mechanical alloying and milling," Prog. Mater. Sci., vol. 46, no. 1–2, pp. 1–184, 2001, doi: 10.1016/S0079-6425(99)00010-9.

[55] P. Baláž, Mechanochemistry in Nanoscience and Minerals Engineering. Berlin: Springer, 2008.

[56] A. Gago-Duport, P. Briones, R. Rodríguez, and M. Covelo, "Amorphous calcium carbonate biomineralization in the earthworm's calciferous gland: Pathways to the formation of crystalline phases," J. Struct. Biol., vol. 162, no. 3, pp. 422–435, 2008, doi: 10.1016/j.jsb.2008.02.008

[57] L. Addadi, S. Raz, and S. Weiner, "Taking advantage of disorder: Amorphous calcium carbonate and its roles in biomineralization," Adv. Mater., vol. 15, no. 12, pp.

959–970, 2003, doi: 10.1002/adma.200300381.

[58] S. Weiner and P. M. Dove, “An overview of biomineralization processes and the problem of the vital effect,” Rev. Mineral. Geochem., vol. 54, no. 1, pp. 1–29, 2003, doi: 10.2113/0540001.

[59] Z. Chen, J. Cao, J. Lu, H. Zhang, and R. Xu, “Biomineralization-inspired material design for environmental remediation,” Acc. Chem. Res., vol. 49, no. 4, pp. 442–451, 2016, doi: 10.1021/acs.accounts.5b00518.

[60] D. A. Long, The Raman Effect: A Unified Treatment of the Theory of Raman Scattering by Molecules. Chichester: Wiley, 2002.

[61] J. R. Ferraro, K. Nakamoto, and C. W. Brown, Introductory Raman Spectroscopy, 2nd ed. San Diego: Academic Press, 2003.

[62] P. U. P. A. Gilbert, R. Abrecht, and C. S. Frazer, “The organic–mineral interface in biominerals,” Rev. Mineral. Geochem., vol. 59, no. 1, pp. 157–185, 2005, doi: 10.2138/rmg.2005.59.7.

[63] D. Cialla-May, X. Zheng, K. Weber, P. Popp, and J. Popp, “Surface- enhanced Raman spectroscopy (SERS): Progress and trends,” Anal. Bioanal. Chem., vol. 409, no. 27, pp. 641–657, 2017, doi: 10.1007/s00216-017-0180-z.

[64] E. Forgacs, T. Cserháti, and G. Oros, “Removal of synthetic dyes from wastewaters: A review,” Environ. Int., vol. 30, no. 7, pp. 953–971, 2004, doi: 10.1016/j.envint.2004.02.001.

[65] M. Komárek, V. Chrastný, and D. Tlustos, “Contamination of vineyard soils with fungicides: A review of environmental and toxicological aspects,” Environ. Int., vol. 36, no. 1, pp. 138–151, 2010, doi: 10.1016/j.envint.2009.10.005.

[66] Z. Li, Y. Deng, X. Li, R. Ding, and Q. Tang, “Phosphate adsorption by calcined oyster shell powders: Mechanisms and performance,” J. Environ. Manage., vol. 196, pp. 476–484, 2017, doi: 10.1016/j.jenvman.2017.03.050.

[67] J. Jehlička and H. G. M. Edwards, “Raman spectroscopy as a tool for the non-

destructive identification of organic minerals in the geological record," Org. Geochem., vol. 39, no. 4, pp. 371–386, 2008, doi: 10.1016/j.orggeochem.2008.01.018.

[68] P. Baláž, Mechanochemistry in Nanoscience and Minerals Engineering.
Berlin: Springer, 2008.

[69] E. Kočišová and A. Kuižová, "Drop coating deposition Raman spectroscopy for bioanalytical applications," Appl. Spectrosc. Rev., 59(8), 717 – 731, 2024, doi:10.1080/05704928.2024.2314534.

[70] R. A. Halvorson and P. J. Vikesland, "Drop coating deposition Raman (DCDR) for microcystin-LR identification and quantitation," Environ. Sci. Technol., 45(13), 5644–5651, 2011, doi:10.1021/es200255y.

[71] C. Ortiz, D. Zhang, Y. Xie, A. Ribbe, and D. Ben-Amotz, "Validation of the drop coating deposition Raman method for protein detection," Anal. Chem., 78(8), 2859–2865, 2006, doi:10.1021/ac0602053.

[72] L. R. Terry, K. P. Johnston, and P. B. Johnson, "Applications of surface- enhanced Raman spectroscopy in environmental contaminant monitoring," Environ. Sci.: Processes Impacts, 24(3), 432–453, 2022, doi:10.1039/D1EM00376A.

[73] J. Jehlička, "Potential and limits of Raman spectroscopy for carotenoid biomarkers in microorganisms," Philos. Trans. R. Soc. A, 372(2029), 20140199, 2014, doi:10.1098/rsta.2014.0199.

[74] J. Robinson and A. J. Szy, "Raman spectroscopy of microbial pigments: β-carotene detection in cyanobacteria," Appl. Environ. Microbiol., 80(5), 1531 – 1539, 2014, doi:10.1128/AEM.00699-14.

[75] F. Nekvapil, M. Venter, I. Brezestean, and S. Cîntă Pînzaru, "Single-cell Raman microspectroscopy for carotenoid stress responses in cyanobacteria," J. Raman Spectrosc., 52(7), 1074–1083, 2021, doi:10.1002/jrs.6101.

[76] B. D. Cullity and S. R. Stock, Elements of X-ray Diffraction, 3rd ed. Upper Saddle River, NJ: Prentice Hall, 2001.

[77] W. H. Bragg and W. L. Bragg, “The reflection of X-rays by crystals,” Proc. R. Soc. Lond. A, vol. 88, no. 605, pp. 428–438, 1913.

[78] C. Hammond, The Basics of Crystallography and Diffraction, 4th ed. Oxford: Oxford University Press, 2015.

[79] H. P. Klug and L. E. Alexander, X-ray Diffraction Procedures: For Polycrystalline and Amorphous Materials, 2nd ed. New York: Wiley, 1974.

[80] R. Jenkins and R. Snyder, Introduction to X-ray Powder Diffractometry. New York: Wiley, 1996.

[81] Y. Xu, J. Zhou, “A practical approach to quantitative analytical surface-enhanced Raman spectroscopy,” Chem. Sci., (to appear) 2025, doi:10.1039/d4cs00861h.

[82] P. A. Mosier-Boss, “Review of SERS substrates for chemical sensing,” Nanomaterials, 7(6), 142, 2017, doi:10.3390/nano7060142.

[83] G. Bodelón, I. Pastoriza-Santos, “Recent progress in surface-enhanced Raman scattering for detection of chemical contaminants in water,” Front. Chem., 8, 478, 2020, doi:10.3389/fchem.2020.00478.

[84] R. Al-Tohamy, et al., “A critical review on the treatment of dye-containing wastewater: Azo dye removal techniques and mechanisms,” J. Hazard. Mater., 424, 127691, 2022.

[85] K. Ramamurthy, “Hues of risk: investigating genotoxicity and environmental impact of azo dyes,” Environ. Pollut. (2024).

[86] An overview of azo dyes environmental impacts, GSC Online Press, 2025.

List of Publications

- **Ilirjana Bajama**, Karlo Maškarić, Geza Lazar, Tudor Tamaş, Codruţ Costinaş, Lucian Barbu-Tudoran, Simona Cîntă Pinzaru.

Aged Biogenic Carbonates from Crustacean Waste: Structural and Functional Evaluation of Calibrated Fine Powders and Their Conversion into Phosphate Minerals.

Materials 2025, 18, 5119. https://doi.org/10.3390/ma18225119

AIS: 0.534 ; IF: 3.7 ; Quartile: Q2

- Csilla Molnár , Karlo Maškarić, Lucian Barbu - Tudoran, Tudor Tămaș, **Ilirjana Bajama**, Simona Cîntă Pînzaru.

SERS Detection of Environmental Variability in Balneary Salt Lakes During Tourist Season: A Pilot Study.

Biosensors 2025, 15, 655. https://doi.org/10.3390/bios15100655

AIS: 0.852 ; IF:6.2 ; Quartile: Q1

- Molnár, C.; Drigla, T.D.; Barbu-Tudoran, L.**; Bajama, I**; Curean, V.; Cîntă Pînzaru, S.

Pilot SERS Monitoring Study of Two Natural Hypersaline Lake Waters from a Balneary Resort during Winter-Months Period.

Biosensors 2024, 14, 19. https://doi.org/10.3390/bios14010019

AIS: 0.861 ; IF: 5.6 ; Quartile: Q1

- Geza Lazar, Tudor Tămaş, Lucian Barbu-Tudoran, Monica M.Venter, **Ilirjana Bajama**, and Simona Cintă Pinzaru.

Biowaste Valorisation: Conversion of Crab Shell-Derived Mg-Calcite into Calcium Phosphate Minerals Controlled by Raman Spectroscopy.

Processes 2025, 13, 3413. https://doi.org/10.3390/pr13113413

AIS: 0.477 ; IF: 3.4 ; Quartile: Q3

Total: AIS: 2.724 ; IF: 18.9 ;

Conference Contributions

Fine powders from aged waste: pollutant adsorbents or new, enriched phosphate minerals? Raman tools to decide. **Ilirjana Bajama**, Karlo Maskaric, Geza Lazar, Tudor Tamas, Codrut Costinas , Lucian-Barbu Tudoran, Supervisor Prof. Dr. Simona Pinzaru Oral: RamanFest 2025, Frankfurt, Germany 2-3 July 2025
https://www.ramanfestconf.com/2025/Abstracts/2025_Bajama_Ilirjana_11.pdf

Marine biowaste-derived materials for medical applications. Iuliana-Cornelia Poplacean, Karlo Maskaric, Geza Lazar, Ilirjana Bajama, Tudor Tamas, Lucian Barbu-Tudoran, Simona Cinta Pinzaru. Poster: Cluj Innovation Days, Cluj-Napoca, Romania 29-30 May 2025
https://2025.clujinnovationdays.com/agenda/

Multiplexed SERS for wastewater treatment utilizing highly absorbent biogenic powders to eliminate environmentally realistic mixtures comprising inorganic pollutants. **Ilirjana Bajama**, Geza Lazar, Tudor-Liviu Tamas, Simona Cinta Pinzaru. Poster: ICORS 2024, Rome, Italy 28 July - 2 August 2024.
https://icors2024.org/wp-content/uploads/2024/08/ICORS2024_Abstracts_oral_and_poster_FINAL_compressed.pdf

Raman technology for the development of a novel biogenic calcite based bone substitute material. Geza Lazar, **Ilirjana Bajama**, Tudor Tamas, Simona Pinzaru. Accepted abstract. Poster: ICORS 2024. Rome, Italy 28 July - 2 August 2024.

https://icors2024.org/wp-content/uploads/2024/08/ICORS2024_Abstracts_oral_and_poster_FINAL_compressed.pdf

Dual-tag paradigm in SERS analysis for removal of antibiotics and dyes from waste water treated with biogenic carbonate powder nanoparticles.**Ilirjana Bajama**, Geza Lazar, Fran Nekvapil, Tudor Tămaș, Lucian Barbu-Tudoran, Simona Cîntă Pînzaru, Poster: ICAVS 12, Krakow, Poland , 27th August – 1st of September 2023

Doxycycline hyclate loaded in porous biogenic carbonate: new drug formulation and characterization using SERS techniques and XRD. **Ilirjana Bajama**, Geza Lazar, Tudor Tămaș, Simona Cîntă Pînzaru, Poster: ICPAM 14, Dubrovnik, Croatia 7-16 September 2022 https://icpams.com/main/wp-content/uploads/BoA-ICPAM14-webfriendly.pdf

Effects of ocean acidification on the morphology and structure of Hexaplex trunculus sea snail shell biomaterial revealed by Raman, XRD AND SEM-EDX data. G. Lazar, F. Nekvapil, **I. Bajama**, T. Tamas, M. Suciu, L. BarbuTodoran, S. Grdan, S. Cinta Pinzaru, S. Dupont, A. Bratos Cetinic, L. Glamuzina. Oral presentation: ICPAM 14, Dubrovnik, Croatia 7-16 Septembrer 2022.
https://icpams.com/main/wp-content/uploads/BoA-ICPAM14-webfriendly.pdf

New biocomposites from waste materials S. Cinta Pinzaru, G. Lazar, F. Nekvapil, R. Hirian, T. Tamas, L. Barbu-Tudoran, M. Suciu, M. Aluas, **I. Bajama**, D. A. Dumitru, S. Tomsic, B. Glamuzina. . ICPAM 14, Dubrovnik, Croatia 7-16 Septembrer 2022.
https://icpams.com/main/wp-content/uploads/BoA-ICPAM14-webfriendly.pdf